arXiv:cond-mat/0610015v3 [cond-mat.stat-mech] 8 Apr 2010

Perturbative renormalization of the Ginzburg–Landau model revisited

J. Kaupužs *
Institute of Mathematics and Computer Science, University of Latvia
29 Raiņa Boulevard, LV–1459 Riga, Latvia

April 9, 2010

Abstract

The perturbative renormalization of the Ginzburg–Landau model is reconsidered based on the Feynman diagram technique. We derive renormalization group (RG) flow equations, exactly calculating all vertices appearing in the perturbative renormalization of the φ^4 model up to the ε^3 order of the ε-expansion. In this case, the φ^2, φ^4, φ^6, and φ^8 vertices appear. All these are relevant in the sense that they do not vanish at the fixed point. We have tested the expected basic properties of the RG flow, such as the semigroup property. Under repeated RG transformation R_s, appropriately represented RG flow on the critical surface converges to certain s–independent fixed point. The Fourier–transformed two–point correlation function $G(\mathbf{k})$ has been considered. Although the ε-expansion of $X(\mathbf{k}) = 1/G(\mathbf{k})$ is well defined on the critical surface, we have revealed a fundamental inconsistency of the perturbative method with the exact rescaling of $X(\mathbf{k})$, represented as an expansion in powers of k at $k \to 0$. We discuss also certain paradox, related to the ε-expansion of $X(\mathbf{k})$ above the critical point. Apart from the ε–expansion, we have tested also a modified approach, where the φ^4 coupling constant u is the expansion parameter at a fixed spatial dimensionality d. Our tests point to some internal inconsistency of such a method.

Keywords: renormalization group, ε-expansion, critical phenomena

*E–mail: kaupuzs@latnet.lv

1 Introduction

The perturbative renormalization of the Ginzburg–Landau (or φ^4) model has a long history (see [1, 2, 3, 4] and references therein). However, as mentioned in [2], a complete formulation of the renormalization group (RG) beyond the ε^2 order of the ε-expansion (where $\varepsilon = 4 - d > 0$, d being the spatial dimensionality) met mathematical difficulties, which could not be overcome. In fact, the ε-expansion of the critical exponents beyond the lowest orders is based on an alternative approach, which relies on the Callan-Symanzik equation [5, 6, 7]. The latter one represents a scaling property of the φ^4 model [5], and the method is based on a set of assumptions [7]. Since the perturbative RG theory is not rigorous, stringent tests of its validity and consistency make sense. Our aim is to perform such tests.

We have tested the expected basic properties of the RG flow. Following the idea in [8], we have checked the semigroup property $R_{s_1 s_2}\mu = R_{s_2} R_{s_1}\mu$, where R_s is the RG operator with scale factor $s > 1$ acting on the set of Hamiltonian parameters μ. We have tested the expected s–independence of the fixed point μ^*, as well as the scaling of the Fourier–transformed two–point correlation function $G(\mathbf{k})$ on the critical surface.

Another strategy of verification has been used in [9], considering a four–dimensional ($d = 4$) model with Gaussian measure modified in such a way to simulate $d = 4 - \varepsilon$ dimensions with ε small and positive. This method allows to control rigorously the remainder of the perturbation series. The obtained results [9] confirm the existence of the non–Gaussian fixed point at a distance $\mathcal{O}(\varepsilon)$ away from the Gaussian one as proposed earlier [1] by the ε–expansion. However, the expected decay of the two–point correlation function appears to be canonical (i. e., Gaussian, see Introduction part in [9]) in disagreement with that provided by the ε–expansion and observed in ordinary spin systems of dimensionality $d < 4$ like, e. g., three–dimensional and two–dimensional Ising models. In view of these observations, the classical (used in the ε–expansion) way of introduction of noninteger spatial dimensionality d via an analytic continuation from d–dimensional hypercubes appears to be more meaningful than that in [9]. In fact, there is no unique definition of the noninteger d. It can be introduced in a more physical way as a suitable "fractal" dimension of an irregular lattice [10, 11].

2 Diagrammatic formulation of the renormalization

As a starting point, we consider a φ^4 model with the Hamiltonian H defined by

$$H/T = \int \frac{r}{2}\varphi^2(\mathbf{x}) + \frac{c}{2}(\nabla\varphi(\mathbf{x}))^2 + \frac{1}{8}\int\int \varphi^2(\mathbf{x}_1)u(\mathbf{x}_1 - \mathbf{x}_2)\varphi^2(\mathbf{x}_2)d\mathbf{x}_1 d\mathbf{x}_2 \ , \tag{1}$$

where the order parameter $\varphi(\mathbf{x})$ is an n–component vector with components $\varphi_i(\mathbf{x})$, depending on the coordinate $\mathbf{x}$, and T is the temperature. The field $\varphi_j(\mathbf{x})$ is given in Fourier representation by $\varphi_j(\mathbf{x}) = V^{-1/2}\sum_{k<\Lambda}\varphi_{j,\mathbf{k}}\, e^{i\mathbf{k}\mathbf{x}}$, where $V = L^d$ is the volume of the system, d is the spatial dimensionality, and Λ is the upper cutoff of the wave vectors. The Fourier-transformed Hamiltonian obeys the equation

$$\begin{aligned} -\frac{H}{T} &= -\frac{1}{2}\sum_{i,\mathbf{k}}\left(r + c\mathbf{k}^2\right) \mid \varphi_{i,\mathbf{k}} \mid^2 \\ &- \frac{1}{8}V^{-1}\sum_{i,j,\mathbf{k}_1,\mathbf{k}_2,\mathbf{k}_3} \varphi_{i,\mathbf{k}_1}\varphi_{i,\mathbf{k}_2}u_{\mathbf{k}_1+\mathbf{k}_2}\varphi_{j,\mathbf{k}_3}\varphi_{j,-\mathbf{k}_1-\mathbf{k}_2-\mathbf{k}_3} \ . \end{aligned} \tag{2}$$

In the Feynman diagram technique [2, 12], the second term in (2) is represented by a fourth order vertex 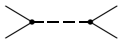 (where field components with vanishing total wave vector are related to the solid lines and the remaining factor — to the dashed line). In the following we will consider only a particular case $u(\mathbf{x}) = u\delta(\mathbf{x})$ or $u_{\mathbf{k}} = u$. The fourth order vertex then can be depicted as by shrinking the dashed line to a point (node). We will mostly use this simplified notation. One has to remember, however, that two of the vertex lines are related to i–th component ($i = 1, \ldots, n$), and the other two lines — to j–th component of a field vector (including the possibility $i = j$). It is shown explicitly in the representation 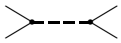 , where these pairs of lines are separated.

In the exact Wilson's RG equation the scale transformation, i. e., the Kadanoff's transformation, is performed by integrating over the Fourier modes with wave vectors obeying $\Lambda/s < k < \Lambda$. It is the first step of the full RG transformation. At this step the transformed Hamiltonian H' is found from the equation

$$e^{-(H'/T)+AL^d} = \int e^{-H/T} \prod_{i,\, \Lambda/s<k<\Lambda} d\varphi_{i,\mathbf{k}} \ , \tag{3}$$

where A is a constant. Note that $\varphi_{i,\mathbf{k}}$ is a complex number and $\varphi_{i,-\mathbf{k}} = \varphi^*_{i,\mathbf{k}}$ holds (since $\varphi_i(\mathbf{x})$ is always real), so that the integration over $\varphi_{i,\mathbf{k}}$ in (3) means in fact the integration over real and imaginary parts of $\varphi_{i,\mathbf{k}}$ for each pair of conjugated wave vectors $\mathbf{k}$ and $-\mathbf{k}$. In practice Eq. (3) cannot be solved exactly. It is done perturbatively, as described in [2]. The perturbation terms can be found more easily by means of the Feynman diagrams.

In the perturbative approach, Hamiltonian is split in two parts $H = H_0 + H_1$, where H_0 is the Gaussian part and H_1 is the rest part considered as a small perturbation. The first and the second term on the right hand side of (2) can be identified with $-H_0/T$ and $-H_1/T$, respectively. Since the term with r also is considered as a small perturbation ($r \sim \varepsilon$ holds in the ε–expansion in $d = 4 - \varepsilon$ dimensions), it is suitable to include it in H_1. In this case diagram expansions are represented by vertices 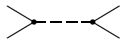 and , where the latter second–order vertex corresponds to the term with r.

It is convenient to normalize Eq. (3) by $Z_s = \int \exp(-\widetilde{H}_0/T) \prod_{i,\, \Lambda/s<k<\Lambda} d\varphi_{i,\mathbf{k}}$, where $\widetilde{H}_0$ is the part of H_0 including only the terms with $\Lambda/s < k < \Lambda$. We have $\ln Z_s = A_s\, L^d$ at $L \to \infty$, where A_s is independent of L, and the normalization yields

$$-\,(H'/T) + (A - A_s)L^d = -(H'_0/T) + \ln\langle \exp(-H_1/T)\rangle_0 \ , \tag{4}$$

where $\langle\cdot\rangle_0$ means the Gaussian average over the field components with $\Lambda/s < k < \Lambda$, whereas H'_0 is the part of H_0 including only the components with $k < \Lambda/s$. Like free energy, $\ln\langle \exp(-H_1/T)\rangle_0$ is represented perturbatively by the sum over all connected Feynman diagrams made of the vertices of $-H_1/T$ by coupling those solid lines, which are associated with wave vectors obeying $\Lambda/s < k < \Lambda$, according to the Wick's theorem. A diagram can contain no coupled lines. There is also a set of diagrams with all lines coupled. The latter diagrams give a constant (independent of $\varphi_{i,\mathbf{k}}$) contribution which compensates the term $(A - A_s)L^d$ in (4). The other contributions correspond to $-H'/T$.

Each term of $\ln\langle \exp(-H_1/T)\rangle_0$ comes from a diagram (or diagrams) of certain topology and is given by a sum over wave vectors which fulfil certain constraints such that $k < \Lambda/s$ holds for uncoupled (external or outer) solid lines, associated with field components $\varphi_{i,\mathbf{k}}$, and $\Lambda/s < k < \Lambda$ holds for coupled solid lines. Besides, the sum of all wave vectors coming into any

of the nodes is zero, and the same index i is related to the solid lines attached to one node of any vertex 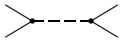 or . The Gaussian average $G_0(\mathbf{k}) = \langle \varphi_{i,\mathbf{k}} \varphi_{i,-\mathbf{k}} \rangle_0 = \langle | \varphi_{i,\mathbf{k}} |^2 \rangle_0$ is related to a coupling line with wave vector $\mathbf{k}$. Here $G_0(\mathbf{k})$ is the Fourier transform of the two–point correlation function in the Gaussian approximation. If only the term with $\mathbf{k}^2$ in (2) is included in H_0/T, then we have $G_0(\mathbf{k}) = 1/(ck^2)$. Including also the term with r, we have $G_0(\mathbf{k}) = 1/(r + ck^2)$, but in this case we need finally to expand $G_0(\mathbf{k})$ in terms of r. The second method yields the same results as the first one: such an expansion generates the same terms, which are obtained in the first method by extending coupling lines in the diagrams originally constructed without vertices to include all possible linear chains made of these vertices. We will use the first, i. e., more diagrammatic method. Note that, when the renormalization procedure is repeated, a continuum of additional vertices appear in the expansion of $-H_1/T$, including ones with explicit wave–vector dependent factors related to the solid lines, which then also have to be taken into account.

In fact, the first step of RG transformation implies the summation over wave vectors of the coupled lines in the diagrams, resulting in a Hamiltonian which depends on $\varphi_{i,\mathbf{k}}$ with $k < \Lambda/s$. The RG transformation has the second step [2]: changing of variables $\tilde{\mathbf{k}} = s\mathbf{k}$ and rescaling the field components $\varphi_{i,\mathbf{k}} \to s^{1-\eta/2} \varphi_{i,\tilde{\mathbf{k}}}$, where η is the critical exponent describing the $\sim k^{-2+\eta}$ singularity of the Fourier–transformed critical two–point correlation function at $k \to 0$. The upper cutoff for the new wave vectors $\tilde{\mathbf{k}}$ is the original one Λ, whereas the density of points in the $\tilde{\mathbf{k}}$–space corresponds to s^d times decreased volume. Therefore we make a substitution $\tilde{V} = s^{-d} V$. In the thermodynamic limit we can replace $\tilde{V}$ by V consistently increasing the density of points in the wave vector space. Finally, we set $\tilde{\mathbf{k}} \to \mathbf{k}$ and obtain a Hamiltonian in original notations.

3 Renormalization up to the order of ε^2

3.1 RG flow equations

Here we consider RG flow equations including all terms up to the order $\mathcal{O}\left(\varepsilon^2\right)$, starting with the renormalization of the coupling constant u. In fact, this is the lowest order of the theory, since it allows to find the fixed point value u^* up to the order of ε. Our aim is to show that we can easily recover the known results using the diagrammatic approach described in Sec. 2. It allows also to write down unambiguously (i. e., without intermediate approximations) the formulae for all perturbation terms.

Important statements here are that the renormalized values of r and u are quantities of order $\mathcal{O}(\varepsilon)$. Besides, $\eta = \mathcal{O}\left(\varepsilon^2\right)$ holds within the ε–expansion and, for any finite renormalization scale s, the variation of c is of order $\mathcal{O}\left(\varepsilon^2\right)$ [2]. Hence, performing the RG transformation R_s with a finite s, the only diagrams of $\ln\langle \exp(-H_1/T) \rangle_0$ contributing to the renormalized coupling constant up to the order of ε^2 are and (this statement can be verified in detail based on a complete renormalization discussed further on). The first one provides the original φ^4 term in Eq. (2), which is merely renormalized by factor $s^{\varepsilon-2\eta}$ at the second step of the RG transformation. The second diagram, which is constructed of two vertices , yields

$$\to \; s^{\varepsilon-2\eta} \left(\frac{u}{8c}\right)^2 V^{-1} \sum_{i,j,\mathbf{k}_1,\mathbf{k}_2,\mathbf{k}_3} \varphi_{i,\mathbf{k}_1} \varphi_{i,\mathbf{k}_2} \varphi_{j,\mathbf{k}_3} \varphi_{j,-\mathbf{k}_1-\mathbf{k}_2-\mathbf{k}_3} \times$$
$$\times [(4n+16)\, Q((\mathbf{k}_1+\mathbf{k}_2)/s, s) + 16\, Q((\mathbf{k}_1+\mathbf{k}_3)/s, s)] \; . \qquad (5)$$

Here Q is given by

$$Q(\mathbf{k},s) = \frac{1}{(2\pi)^d} \int\limits_{\Lambda/s<q<\Lambda} q^{-2} \mid \mathbf{k}-\mathbf{q} \mid^{-2} \mathcal{F}(\mid \mathbf{k}-\mathbf{q} \mid, s) d^d q \ , \tag{6}$$

where $\mathcal{F}(k,s) = 1$ if $\Lambda/s < k < \Lambda$, and $\mathcal{F}(k,s) = 0$ otherwise. To obtain this result, we have deciphered the 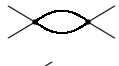 diagram as a sum of three diagrams of different topologies made of vertices 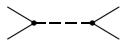 , i. e., 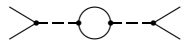 , 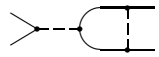 , and 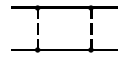 , providing the same topological picture when shrinking the dashed lines to points. Note that any loop made of solid lines of 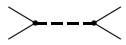 gives a factor n, and one needs also to compute the combinatorial factors (see, e. g., [2, 12]). For the above three diagrams, the resulting factors are $4n$, 16, and 16, which enter the prefactors of Q in (5).

Quantity $Q(\mathbf{k}/s,s)$ has a constant contribution

$$Q(\mathbf{0},s) = K_d \, \Lambda^{-\varepsilon}(s^{\varepsilon}-1)/\varepsilon \ , \tag{7}$$

as well as a $\mathbf{k}$–dependent correction $\Delta(k,s) = Q(\mathbf{k}/s,s) - Q(\mathbf{0},s)$ vanishing at $k=0$. Here $K_d = S(d)/(2\pi)^d$, where $S(d) = 2\pi^{d/2}/\Gamma(d/2)$ is the area of unit sphere in d dimensions.

The term provided by the $Q(\mathbf{0},s)$ part of $Q(\mathbf{k}/s,s)$ in (5) is identified with the φ^4 vertex, contributing to the renormalized coupling constant u'. It is consistent with the general form

$$V^{-1} \sum_{i,j,\mathbf{k}_1,\mathbf{k}_2,\mathbf{k}_3} \bar{Q}\left(\mathbf{k}_1,\mathbf{k}_2,\mathbf{k}_3,s,n,\varepsilon\right) \varphi_{i,\mathbf{k}_1}\varphi_{i,\mathbf{k}_2}\varphi_{j,\mathbf{k}_3}\varphi_{j,-\mathbf{k}_1-\mathbf{k}_2-\mathbf{k}_3} \ , \tag{8}$$

of quartic (φ^4) terms, where the contribution corresponding to the ordinary φ^4 vertex is uniquely identified with one provided by the constant part $\bar{Q}\left(\mathbf{0},\mathbf{0},\mathbf{0},s,n,\varepsilon\right)$ of the weight function $\bar{Q}$.

Taking into account also the contribution coming directly from vertex, the RG flow equation reads

$$u' = s^{\varepsilon-2\eta}\left[u - u^2\,\frac{K_d(n+8)}{2c^2\Lambda^{\varepsilon}} \times \frac{s^{\varepsilon}-1}{\varepsilon}\right] + \mathcal{O}\left(\varepsilon^3\right) \ , \tag{9}$$

where u' is the renormalized and u is the original coupling constant. The expansion in ε yields the well known equation [2]

$$u' = u + \varepsilon u \, \ln s - u^2 \, B \, \ln s + \mathcal{O}\left(\varepsilon^3\right) \ , \tag{10}$$

where $B = K_4(n+8)/(2c^2)$, with the known fixed–point value at $u = u^* = B^{-1}\varepsilon + \mathcal{O}\left(\varepsilon^2\right)$.

The correction term $\Delta(k,s)$ changes the renormalized Hamiltonian as follows:

$$\begin{aligned} H/T \ \ \rightarrow \ \ (H/T) - s^{\varepsilon-2\eta}\left(\frac{u}{2c}\right)^2 V^{-1} \sum_{i,j,\mathbf{k}_1,\mathbf{k}_2,\mathbf{k}_3} \varphi_{i,\mathbf{k}_1}\varphi_{i,\mathbf{k}_2}\varphi_{j,\mathbf{k}_3}\varphi_{j,-\mathbf{k}_1-\mathbf{k}_2-\mathbf{k}_3} \times \\ \times[(1+n/4)\,\Delta(\mid \mathbf{k}_1+\mathbf{k}_2 \mid, s) + \Delta(\mid \mathbf{k}_1+\mathbf{k}_3 \mid, s)] \ . \end{aligned} \tag{11}$$

It can be represented as a sum of two fourth–order vertices including prefactors $\Delta(\mid \mathbf{k}_1+\mathbf{k}_2 \mid, s)$ and $\Delta(\mid \mathbf{k}_1+\mathbf{k}_3 \mid, s)$, respectively, related to two of the vertex lines.

In the following we will introduce a more suitable diagrammatic notation. In the one-component case $n=1$, the term appearing in (5) is represented as

$$s^{2\varepsilon-2\eta}\,\frac{9}{16}u^2 \tag{12}$$

where is the Feynman diagram in which the Gaussian propagator $1/(ck^2)$ with $k \in [\Lambda, s\Lambda]$ is related to the dotted coupling lines. In other words, the propagator is multiplied with the cut function $\mathcal{F}(k/s, s)$. In general (also for other diagrams considered in our paper), the field components supplied with the factor V^{1-m} are related to $2m$ external lines, the rest of such factors being absorbed in the $\mathbf{k}$–space integrals. An additional s^{ε} factor in (12) comes from the rescaling of wave vectors in such a way that the integration now takes place over $k \in [\Lambda, \Lambda s]$ for the internal lines. This procedure is necessary in order to represent the result as a Feynman diagram with vanishing sum of the wave vectors entering each node.

Subtracting from the $\mathbf{k}$–space integral its value calculated at $\mathbf{k} = \mathbf{0}$ for the external lines, the result is represented as

$$s^{2\varepsilon - 2\eta} \frac{9}{16} u^2 \quad . \tag{13}$$

Similar notation is applied throughout the paper, where the line crossing the diagram indicates the subtraction of zero–$\mathbf{k}$ contribution. The diagram representation of this kind has been proposed in [13]. In the general n–component case, we denote by

$$\Sigma\Big(\quad \Big) = \frac{n}{9} \quad + \frac{4}{9} \quad + \frac{4}{9} \tag{14}$$

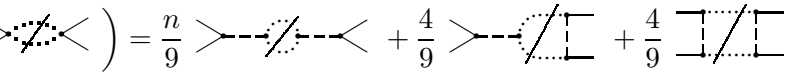

the sum of all such kind of diagrams, which reduce to when the dashed lines shrink to points. In (14) the coefficients are normalized in such a way that their sum is 1 at $n = 1$. Note that in the diagram technique with such vertices, one has to count closed loops made of all kind of lines related to the propagator $1/(ck^2)$. In this notation (11) becomes

$$H/T \to (H/T) - s^{2\varepsilon - 2\eta} u^2 \frac{9}{16} \Sigma\Big(\quad \Big) \tag{15}$$

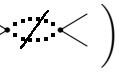

Analogous diagrammatic representation is possible for all vertices appearing in a repeated renormalization. In accordance with such notation, the ordinary φ^4 vertex in (2) will be represented as $-(u/8)$ 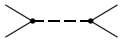 .

For a complete renormalization up to the order of ε^2, one has to take into account also other contributions of this order, including the φ^6 vertex

$$\begin{aligned} \Sigma\Big(\quad \Big) &\equiv \quad \\ &= c^{-1} V^{-2} \sum_{i,j,l,\mathbf{k}_1,\mathbf{k}_2,\mathbf{k}_3,\mathbf{k}_4,\mathbf{k}_5} \varphi_{i,\mathbf{k}_1} \varphi_{i,\mathbf{k}_2} \varphi_{j,\mathbf{k}_3} \varphi_{j,\mathbf{k}_4} \varphi_{l,\mathbf{k}_5} \varphi_{l,-\mathbf{k}_1-\mathbf{k}_2-\mathbf{k}_3-\mathbf{k}_4-\mathbf{k}_5} \\ &\qquad \times \mid \mathbf{k}_1 + \mathbf{k}_2 + \mathbf{k}_3 \mid^{-2} \mathcal{F}(\mid \mathbf{k}_1 + \mathbf{k}_2 + \mathbf{k}_3 \mid /s, s) \end{aligned} \tag{16}$$

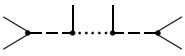

appearing due to the coupling of two vertices , as well as the quadratic term of the general form $(1/2) \sum_{i,\mathbf{k}} \tilde{\theta}(\mathbf{k}) \mid \varphi_{i,\mathbf{k}} \mid^2$ provided by diagrams with two external lines. In the representation $\tilde{\theta}(\mathbf{k}) = r + c\mathbf{k}^2 + \theta(\mathbf{k})$, it corresponds to the φ^2 vertex in (2) with one additional term.

In the rest part of this section we will consider the structure of the renormalized Hamiltonian and the related RG flow equations, providing the proofs afterwards in Sec. 3.2. Thus, the renormalized Hamiltonian has the form

$$\begin{aligned} \frac{H}{T} &= \frac{1}{2} \sum_{i,\mathbf{k}} \Big(r + c\mathbf{k}^2 + \theta(\mathbf{k}) \Big) \mid \varphi_{i,\mathbf{k}} \mid^2 + \frac{u}{8} \\ &+ a_4 \, \Sigma\Big(\quad \Big) + a_6 \, \Sigma\Big(\quad \Big) + \mathcal{O}\left(\varepsilon^3\right) . \end{aligned} \tag{17}$$

Here the wave vectors of the dotted lines are in the interval $[\Lambda, \zeta\Lambda]$, where the parameter ζ has the initial value 1 and is transformed according to

$$\zeta' = s\,\zeta \tag{18}$$

in a process of repeated renormalization. Here ζ is the previous and ζ' is the new (renormalized) value of this parameter after the current RG transformation (RGT) with the scale factor s. The weight coefficients a_4 and a_6 in this order of the ε–expansion obey simple RG flow equations

$$a_4' = -\frac{9u^2}{16} + \mathcal{O}\left(\varepsilon^3\right) \tag{19}$$

$$a_6' = -\frac{u^2}{8} + \mathcal{O}\left(\varepsilon^3\right) \tag{20}$$

relating the new values of these parameters in each RGT to the previous value of u. The initial values of a_4 and a_6 are not important, since the corresponding diagrams vanish at $\zeta = 1$. The RG flow equations for the Hamiltonian parameters u and r read

$$u' = s^{\varepsilon}\left[u - \frac{n+8}{2}u^2\ \mathbf{0}\right] + \mathcal{O}\left(\varepsilon^3\right) \tag{21}$$

$$r' = s^2\left[\left(r + \frac{n+2}{2}u\ \mathbf{0}\right)\left(1 - \frac{n+2}{2}u\ \mathbf{0}\right) - \frac{n+2}{2}\left(u^2\ \mathbf{0} - \frac{16}{3}a_4\ \mathbf{0} - 24a_6\ \mathbf{0}\right)\right] + \mathcal{O}\left(\varepsilon^3\right), \tag{22}$$

where $\mathbf{0}$ is the diagram with amputated four external lines having zero wave vectors, and the other diagrams are defined analogously. The wave vectors of the internal solid lines are in the range $[\Lambda/s, \Lambda]$, whereas those of the dotted lines — in the range $[\Lambda, \Lambda\zeta]$. Eq. (21) is the same as (9), only the irrelevant for this order of the ε–expansion factor $s^{-2\eta}$ is omitted, like also the factor $s^{-\eta}$ in (22). Taking into account (19)–(20) and the fact that u is renormalized only by $\mathcal{O}\left(\varepsilon^2\right)$ in one RGT, the diagram expression in the last line of (22) can be written as $-\frac{1}{2}(n+2)u^2\left(\mathbf{0} + 3\ \mathbf{0} + 3\ \mathbf{0}\right)$.

The parameter c enters all diagrams. In the actual order of the ε–expansion its variation does not produce additional terms in (21) and (22). However, one has to update its value according to the equation

$$c' = s^{-\eta}\left(c - \frac{n+2}{2}\Pi\right) + \mathcal{O}\left(\varepsilon^3\right), \tag{23}$$

where

$$\Pi = \lim_{k\to 0}\frac{D(k) - D(0)}{k^2} \tag{24}$$

with

$$D(k) = u^2\left(\mathbf{k} + 3\ \mathbf{k} + 3\ \mathbf{k}\right). \tag{25}$$

Here the symbol $\mathbf{k}$ indicates the wave vector related to the amputated external line. Finally, the RG flow equation for the function $\theta(\mathbf{k})$ reads

$$\theta'(\mathbf{k}) = s^2\left(\theta(\mathbf{k}/s) - \frac{n+2}{2}\Phi(\mathbf{k}/s)\right) + \mathcal{O}\left(\varepsilon^3\right), \tag{26}$$

where

$$\Phi(\mathbf{k}) = D(k) - D(0) - k^2\Pi \,. \tag{27}$$

Using the diagram technique, the function $\theta(\mathbf{k})$ can be represented as

$$\theta(\mathbf{k}) = -\frac{n+2}{2}u^2 \ \mathbf{k}\ \ + \mathcal{O}\left(\varepsilon^3\right) \ , \tag{28}$$

where the wavy line indicates that both the constant contribution and that proportional to k^2 (with the proportionality coefficient determined at $k \to 0$) are subtracted. Besides, the range of the wave vectors for the internal lines is $[\Lambda, \Lambda\zeta]$, where ζ is determined after the actual RGT.

3.2 Proof of the RG flow equations

In Sec. 3.1 the RG flow equations are given without proof. Their proof consists of a verification that, at each RGT, the Hamiltonian keeps the form (17) in accordance with the given update rules for all parameters. Consider first the φ^6 vertex at $n = 1$, summing up all diagrams of this topology, which appear in H/T at a given RGT:

$$s^{2\varepsilon-3\eta}\left(-\frac{u^2}{8} \ + a_6 \ \right) = -\frac{u^2}{8}\left(\ + \ \right) + \mathcal{O}\left(\varepsilon^3\right)$$
$$= -\frac{u^2}{8} \ + \mathcal{O}\left(\varepsilon^3\right) = a_6' \ + \mathcal{O}\left(\varepsilon^3\right) \ . \tag{29}$$

Here the wave vectors within $[\Lambda, \Lambda s]$, $[\Lambda s, \Lambda\zeta']$, and $[\Lambda, \Lambda\zeta']$ correspond to the solid, dashed, and dotted coupling lines, respectively, where $\zeta' = s\zeta$. (These dashed lines should not be confused with those of .) In (29), the vertex is produced by coupling (and rescaling) two φ^4 vertices , whereas comes from the rescaling of already existing before the given RGT φ^6 vertex. We have omitted the irrelevant for this order of the ε–expansion rescaling factor resulting from the renormalization of parameter c. We have used the substitution $a_6 = -u^2/8 + \mathcal{O}\left(\varepsilon^3\right)$, which holds according to the assumption that our RG flow equation (20) was satisfied and u was changed only by $\mathcal{O}\left(\varepsilon^2\right)$ in the previous RGT. It is true for the first RGT, so that the relations (29) provide the proof of (20) by induction. It is obviously valid for any finite number of RGT.

The generalisation to the n–component case is trivial here, since there is only one way how to couple two vertices to form the sixth-order vertex.

Similarly, the summation of terms provided by the diagrams of topology, subtracting the contribution included in the ordinary φ^4 vertex, gives us

$$s^{2\varepsilon-2\eta}\left(-\frac{9u^2}{16} \ + a_4 \ + 9a_6 \ \right)$$
$$= -\frac{9u^2}{16}\left(\ + \ + 2 \ \right) + \mathcal{O}\left(\varepsilon^3\right)$$
$$= -\frac{9u^2}{16} \ + \mathcal{O}\left(\varepsilon^3\right) = a_4' \ + \mathcal{O}\left(\varepsilon^3\right) \tag{30}$$

with the same k intervals for different coupling lines as in (29). It proves (19) for a finite number m of RG transformations at $n = 1$. Here the three diagrams in the first line of (30)

come from two vertices, rescaling of the already existing vertex with the coefficient a_4, and from the φ^6 vertex via coupling its two lines. Besides, $\equiv$ holds, since the diagram vanishes if the external lines have zero wave vectors. This derivation is easily generalised to the n–component case represented by (17): the same relations, only multiplied with the corresponding weight factors in (14), hold for diagrams of each topology, when is deciphered as the diagrams on the right hand side of (14).

A subtle question here is whether the small corrections, omitted in (29) and (30) at each RGT, do not lead to larger than $\mathcal{O}\left(\varepsilon^3\right)$ deviations from the assumed form of the renormalized Hamiltonian when the number of RG transformations m growth unlimitedly. A rigorous answer to this question can be found, comparing the results of the actual update rules with those provided by a renormalization scheme in which all these corrections are taken into account. Such a scheme will be considered in Sec. 4. Here we note only that the actual RG flow equations are valid within the given accuracy for any m.

The derivation of (21) has been already discussed in Sec. 3.1. Recall that the updated value of the coupling constant u of the ordinary φ^4 vertex is related to the constant part of the weight function in (8), which comes from the rescaled already existing ordinary φ^4 vertex, as well as from other diagrams with four external lines generated in the actual RGT. The coupling of two lines of the vertex 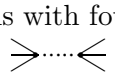 gives vanishing contribution here, so that the coupling is the only relevant one at the order of ε^2. It results in (21).

Similarly, the updated value of the parameter r is identified with the constant part of the weight function $\tilde{\theta}(\mathbf{k})$ in the general representation of the quadratic term $(1/2)\sum\limits_{i,\mathbf{k}}\tilde{\theta}(\mathbf{k})\mid\varphi_{i,\mathbf{k}}\mid^2$, and is generated by the diagrams with two external lines. It results in (22), where the terms with a_4 and a_6 appear via coupling the lines of the vertices and 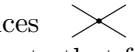 , respectively, whereas other diagrams in (22) are produced by the vertices and .

The RG flow equation (23) for the parameter c is similar to that for r with the only difference that here we single out the contribution to $\tilde{\theta}(\mathbf{k})$, which is proportional to k^2. Subtracting both the constant contribution and that of k^2, we arrive at the equation for $\theta(\mathbf{k})$ (26). Its diagrammatic form (28) is proven by summation of diagrams like, e. g., in Eq. (30).

Finally, we check that all terms up to the order of ε^2 are already included. In particular, the part of (17) with factor $\theta(\mathbf{k})/2$ can be seen as the vertex supplied with such a weight factor. However, its coupling to other vertices gives only a contribution of order $\mathcal{O}\left(\varepsilon^3\right)$. Recall that we do not consider the constant part of Hamiltonian, which is independent of the field configuration and is represented by closed diagrams without external lines.

3.3 Estimation of k–space integrals

It is important to know whether the $\mathbf{k}$–space integrals over the internal lines of the diagrams, appearing in our representation of the renormalized Hamiltonian, are convergent when the RG transformation is repeated unlimitedly many times, i. e., at $\zeta\to\infty$.

First, we note that the diagram in four dimensions, i. e.,

$$= \frac{1}{(2\pi)^4}\int\limits_{\Lambda<q<\Lambda\zeta}\frac{d^4q}{c^2q^4} = \frac{K_4}{c^2}\int\limits_{\Lambda}^{\Lambda\zeta}\frac{dq}{q} = \frac{K_4}{c^2}\ln\zeta \tag{31}$$

diverges when the region $q\in[\Lambda,\Lambda\zeta]$ of wave vectors for the internal lines is extended to $[\Lambda,\infty]$

at $\zeta \to \infty$. Similar diagram, where the zero–$\mathbf{k}$ contribution is subtracted,

$I(k,\zeta) =$ 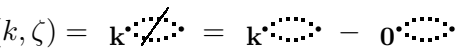

(32)

with $\mathbf{k}$ corresponding to the sum of wave vectors for the two amputated external lines, is convergent at $d = 4$, as well as in $d = 4 - \varepsilon$ dimensions, where we have

$$I(q,\zeta) = \frac{1}{c^2(2\pi)^d} \int\limits_{\Lambda<k<\Lambda\zeta} \left(\frac{\hat{\mathcal{F}}(\mid \mathbf{q}+\mathbf{k} \mid, \zeta)}{k^2 \mid \mathbf{q}+\mathbf{k} \mid^2} - \frac{1}{k^4} \right) d^d k \tag{33}$$

$$= \frac{K_d}{c^2 \int\limits_0^\pi (\sin\theta)^{2-\varepsilon} d\theta} \times \int\limits_\Lambda^{\Lambda\zeta} k^{1-\varepsilon} dk \int\limits_0^\pi \left(\frac{\hat{\mathcal{F}}\left(\sqrt{q^2+2kq\cos\theta+k^2}, \zeta\right)}{q^2+2kq\cos\theta+k^2} - \frac{1}{k^2} \right) (\sin\theta)^{2-\varepsilon} d\theta$$

with $\hat{\mathcal{F}}(k,\zeta) = 1$ if $\Lambda < k < \Lambda\zeta$, and $\hat{\mathcal{F}}(k,\zeta) = 0$ otherwise. The last identity in (33) is true for any integer d, according to the well known formula for integration in spherical coordinates, so that we can put here ε as a continuous parameter in the usual sense of the ε–expansion.

In the following calculations of this subsection, we set $c = 1$ and $\Lambda = 1$ for simplicity. Considering the large–q asymptotic at $\zeta = \infty$, we can set $\hat{\mathcal{F}} = 1$ in (33), which gives correct result up to a term vanishing at $q \to \infty$. Further on, we use the decomposition

$$\frac{1}{k^2 \mid \mathbf{q}+\mathbf{k} \mid^2} - \frac{1}{k^4} = f_0(k,q) + \Delta f(\mathbf{k},\mathbf{q}) \ , \tag{34}$$

where

$$f_0(k,q) = \begin{cases} k^{-2}q^{-2} - k^{-4} & , \quad k < q \\ 0 & , \quad k > q \end{cases} \tag{35}$$

An important property of $\Delta f(\mathbf{k},\mathbf{q})$, defined by (34) and (35), is

$$\int\limits_{k>1} \Delta f(\mathbf{k},\mathbf{q}) d^4k = 0 \qquad \text{at} \quad q \to \infty \ . \tag{36}$$

It is true because

$$\frac{1}{(2\pi)^4} \int\limits_{k>1} \left(\frac{1}{k^2 \mid \mathbf{q}+\mathbf{k} \mid^2} - \frac{1}{k^4} \right) d^4k = \frac{1}{(2\pi)^4} \int\limits_{k>1} f_0(k,q) d^4k = -\ln q + \frac{1}{2} \tag{37}$$

holds at $q \to \infty$. The $-\ln q + 1/2$ asymptotic is evident for the second integral. For the first one, it is verified by integration over k (via the substitution $p = k + q\cos\theta$) and then – over the angle θ in spherical coordinates. According to the decomposition (34), we have

$$I(q,\infty) = K_d \left\{ \frac{q^{-\varepsilon}}{2-\varepsilon} - \frac{1-q^{-\varepsilon}}{\varepsilon} \right\} + \Delta I(q) \qquad \text{at} \quad q \to \infty \ , \tag{38}$$

where the term $K_d \{\cdot\}$ is the contribution of $f_0(k,q)$, whereas $\Delta I(q)$ comes from $\Delta f(\mathbf{k},\mathbf{q})$ and is equal to

$$\Delta I(q) = \frac{K_d \, \Gamma[(4-\varepsilon)/2]}{\sqrt{\pi}\, \Gamma[(3-\varepsilon)/2]} \times \int\limits_1^\infty k^{-1-\varepsilon} dk \int\limits_0^\pi \Delta \widetilde{f}(k/q,\theta) (\sin\theta)^{2-\varepsilon} d\theta \ , \tag{39}$$

where

$$\Delta\widetilde{f}(x,\theta) = \frac{x^2}{1+2x\cos\theta+x^2} - 1 + \left(1-x^2\right)\Theta(1-x)\ . \tag{40}$$

Here $\Theta(x)$ denotes the theta step function, and the known identity

$$\int\limits_0^\pi (\sin\theta)^x d\theta = \sqrt{\pi}\,\frac{\Gamma\left(\frac{x+1}{2}\right)}{\Gamma\left(\frac{x+2}{2}\right)} \tag{41}$$

has been used to obtain (39). According to (36), $\Delta I(q)$ vanishes at $d=4$. Using this property, from (39) we obtain

$$\Delta I(q) = \frac{2}{\pi} K_d\,\mathcal{A}\,\left(-\varepsilon+\varepsilon^2\ln q\right) + \widetilde{c}\,\varepsilon^2 + \mathcal{O}\left(\varepsilon^3\right)\ , \tag{42}$$

where

$$\mathcal{A} = \int\limits_0^\infty \frac{\ln x}{x}\,dx \int\limits_0^\pi \Delta\widetilde{f}(x,\theta)\sin^2\theta\,d\theta + \int\limits_0^\infty \frac{dx}{x}\int\limits_0^\pi \Delta\widetilde{f}(x,\theta)\sin^2\theta\,\ln(\sin\theta)d\theta \tag{43}$$

and $\widetilde{c}$ is a constant at $q\to\infty$. According to (38) and (42), we have

$$\begin{aligned} I(q,\infty) &= K_d\left[-\ln q + \frac{1}{2} + \frac{\varepsilon}{2}\left(\ln^2 q - \ln q\right) + \left(\frac{1}{4} - \frac{2\mathcal{A}}{\pi}\right)\left(\varepsilon - \varepsilon^2\ln q\right)\right. \\ &+ \left.\frac{\varepsilon^2}{12}\left(-2\ln^3 q + 3\ln^2 q\right) + \hat{c}\,\varepsilon^2\right] + \mathcal{O}\left(\varepsilon^3\right) \qquad \text{at} \quad q\to\infty\ , \end{aligned} \tag{44}$$

where $\hat{c}$ is a constant.

In a more general case, for $I(q,\zeta)$ we obtain

$$I(q,\zeta) = I(q,\infty) + \delta I(q,\zeta)\ , \tag{45}$$

where $\delta I(q,\zeta)$ has the asymptotic form

$$\delta I(q,\zeta) = q^{-\varepsilon}\hat{f}(\zeta/q,\varepsilon) \qquad \text{at} \quad q,\zeta\to\infty\ , \tag{46}$$

where

$$\begin{aligned} \hat{f}(y,\varepsilon) &= -\frac{K_d\,\Gamma[(4-\varepsilon)/2]}{\sqrt{\pi}\,\Gamma[(3-\varepsilon)/2]}\left\{\int\limits_0^y x^{-1-\varepsilon}dx \int\limits_0^\pi \frac{x^2\,\Theta(1+2x\cos\theta+x^2-y^2)}{1+2x\cos\theta+x^2}\,(\sin\theta)^{2-\varepsilon}d\theta\right. \\ &+ \left.\int\limits_y^\infty x^{-1-\varepsilon}dx \int\limits_0^\pi \left(\frac{x^2}{1+2x\cos\theta+x^2} - 1\right)(\sin\theta)^{2-\varepsilon}d\theta\right\}\ . \end{aligned} \tag{47}$$

Based on these results, we can evaluate the large–$\mathbf{q}$ (i. e., $C<q<\zeta$ for large enough C at a given k) contribution to the diagram in four dimensions as

$$\frac{1}{(2\pi)^4}\int\limits_{C<q<\zeta}\left[I(|\,\mathbf{k}+\mathbf{q}\,|,\zeta) - I(q,\zeta)\right]q^{-2}d^4q\ . \tag{48}$$

It, in fact, diverges at $\zeta \to \infty$, and the divergent part comes from the $-K_4 \ln q$ term in $I(q,\infty)$, providing the contribution

$$-\frac{K_4^2}{\pi}\int\limits_C^{\zeta} q\,dq \int\limits_0^{\pi} \ln\left(1+\frac{2kq\cos\theta+k^2}{q^2}\right)\sin^2\theta\,d\theta\ . \tag{49}$$

Using the expansion in powers of k/q, we see that (49) logarithmically diverges at $\zeta \to \infty$. However, if we subtract the term $\propto k^2$, the result is convergent. It implies that the diagram appearing in (28) has finite value at $\zeta \to \infty$.

Similarly, we can treat the large–wave–vector contribution to the diagram further considered in the renormalization up to the order of ε^3. This graph contains the subtraction of the zero–vector contribution from the internal block , as well as from the whole diagram. It is defined (at $c=\Lambda=1$) by

$$= \frac{1}{(2\pi)^4}\int\limits_{1<q_1<\zeta} \left\{q_1^{-2}\mid \mathbf{q}_1+\mathbf{k}\mid^{-2}\hat{\mathcal{F}}(\mid \mathbf{q}_1+\mathbf{k}\mid,\zeta)\,I(\mid \mathbf{q}-\mathbf{q}_1\mid,\zeta)-q_1^{-4}I(q_1,\zeta)\right\}d^4q_1 \tag{50}$$

in four dimensions. Using the asymptotic estimates of $I(q,\infty)$ and $\delta I(q,\zeta)$, we find that the tail of large q_1 is convergent for any given $\mathbf{k}$ and $\mathbf{q}$.

The actual integrals (49) and (50) have been estimated in four dimensions ($d=4$). Those ones, which are convergent at $d=4$, are convergent also in $d=4-\varepsilon$ dimensions for small (positive and also negative) ε when considering the $\mathbf{k}$–space integrals as continuous functions of d in the usual sense of the ε–expansion. It is because the contribution of large wave vectors changes only slightly.

3.4 Testing the semigroup property

Here we test the semigroup property

$$R_{s_1 s_2}\mu = R_{s_2}R_{s_1}\mu \tag{51}$$

discussed already in Sec. 1. In fact, we verify that the renormalized Hamiltonian after two subsequent RGT with scale factors s_1 and s_2 is the same as after one RGT with the scale factor $s_1 s_2$. It can be seen most easily for the vertices 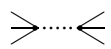 and , as consistent with Eqs. (18) to (20) and the fact that u is renormalized only by an amount of $\mathcal{O}\left(\varepsilon^2\right)$. The semigroup property for the coupling constant u easily follows from (21). After the first RGT we have

$$u' = s_1^{\varepsilon}\left[u-\frac{n+8}{2}u^2\ \mathbf{0}\right] + \mathcal{O}\left(\varepsilon^3\right)\ , \tag{52}$$

where the dotted line refers to the k interval $[\Lambda/s_1,\Lambda]$. After the second RGT the value of the coupling constant, denoted as u'', becomes

$$u'' = s_2^{\varepsilon}\left[u'-\frac{n+8}{2}u'^2\,s_1^{-\varepsilon}\ \mathbf{0}\right] + \mathcal{O}\left(\varepsilon^3\right)\ , \tag{53}$$

where the dashed line refers to the interval $[\Lambda/(s_1 s_2), \Lambda/s_1]$. Here the rescaling of the wave vectors from $k \in [\Lambda/s_2, \Lambda]$ to $k \in [\Lambda/(s_1 s_2), \Lambda/s_1]$ has been performed for convenience. Inserting (52) in (53), and taking into account that $u = \mathcal{O}(\varepsilon)$, we obtain

$$
\begin{aligned}
u'' &= (s_1 s_2)^{\varepsilon} \left[u - \frac{n+8}{2} u^2 \left\{ \mathbf{0} \cdots + \mathbf{0} \cdots \right\} \right] + \mathcal{O}\left(\varepsilon^3\right) \\
&= (s_1 s_2)^{\varepsilon} \left[u - \frac{n+8}{2} u^2 \ \mathbf{0} \cdots \right] + \mathcal{O}\left(\varepsilon^3\right) \ ,
\end{aligned}
\tag{54}
$$

where $k \in [\Lambda/(s_1 s_2), \Lambda]$ corresponds to the solid coupling lines. It is obvious that (54) is identical to the result of one RGT obtained from (21) with $s = s_1 s_2$, which proves the semigroup property. Analogous diagram summation proves this property also in the next order of the ε–expansion [13].

The semigroup property for the parameter r, when performing the RG transformations of the initial Hamiltonian with $\zeta = 1$, is proven straightforwardly by the same method. Namely, the result of the second RGT (applying (22)) is represented by the diagrams containing the dotted and the dashed lines with $k \in [\Lambda/s_1, \Lambda]$ and $k \in [\Lambda/(s_1 s_2), \Lambda/s_1]$, respectively. These diagrams sum up to give ones with $k \in [\Lambda/(s_1 s_2), \Lambda]$, which correspond to those of the one–step renormalization with $s = s_1 s_2$. In distinction to the case of u, here more complicated terms appear, including different lines in one diagram. The situation is less trivial when starting with $\zeta > 1$. In this case all diagrams can be decomposed in such ones, which contain three types of lines with $k \in [\Lambda, \Lambda\zeta]$, $k \in [\Lambda/s_1, \Lambda]$ and $k \in [\Lambda/(s_1 s_2), \Lambda/s_1]$, respectively. Then we prove the semigroup property by checking that such diagram representation for the two–step renormalization is identical (up to the considered order of the ε–expansion) to that for the one–step renormalization. The semigroup property for the parameters c and $\theta(\mathbf{k})$ is proven by this method, as well.

3.5 The fixed point

The RG flow described by the truncated perturbative equations of Sec. 3.1 has certain fixed point as a steady state solution of the RG flow equations. We shall mark the fixed–point values by an asterisk, except the value of c, since the fixed point exists for any given c, as it will be seen from the following analysis. The fixed–point value of the coupling constant u, i. e.,

$$
u^* = \frac{2c^2}{(n+8)K_4} \, \varepsilon + \mathcal{O}\left(\varepsilon^2\right) \tag{55}
$$

has been already mentioned in Sec. 3.1. According to (19) and (20), we have $a_4^* = -(9u^{*2})/16 + \mathcal{O}(\varepsilon^3)$ and $a_6^* = -u^{*2}/8 + \mathcal{O}(\varepsilon^3)$. It is generally expected that the fixed point is independent of the scale parameter s. In the exact renormalization, it is a consequence of the semigroup property. In the perturbation theory, it is expected to hold at each order of the expansion. The above considered fixed–point values obey this requirement within the given accuracy. It is obviously true also for the r^* value in the lowest order of the expansion, i. e.,

$$
r^* = -\frac{c\Lambda^2}{2} \, \frac{n+2}{n+8} \, \varepsilon + \mathcal{O}\left(\varepsilon^2\right) \ . \tag{56}
$$

However, it is less obvious for the next–order correction to r^*, as well as for other parameters of the fixed–point Hamiltonian. Therefore, we have performed some tests. Using (55), (19),

and (20), we find from (22) that r^* is independent of s within the error of $\mathcal{O}\left(\varepsilon^3\right)$ if u^* is s–independent up to the ε^2 order and

$$f(s) = -\frac{3}{2}\frac{K_4^2\Lambda^2}{c^3}\,\ln s + const\cdot\left(s^2-1\right) \tag{57}$$

holds, where

$$f(s) = s^2\Bigg(\ \mathbf{0}\ \ +3\ \mathbf{0}\ \ +3\ \mathbf{0}\ \ \Bigg)\ . \tag{58}$$

Here the solid lines have wave vectors within $k\in[\Lambda/s,\Lambda]$, whereas the dotted lines – within $k\in[\Lambda,\Lambda\zeta]$ at $\zeta\to\infty$, and all terms are evaluated at $d=4$. On the other hand, we prove that the function (58) obeys the equation

$$s_2^2 f(s_1) + f(s_2) = f(s_1 s_2) - 3\ \mathbf{0}\ \ \times\ \ \mathbf{0}\ \ \times (s_1 s_2)^2\ , \tag{59}$$

where the dashed lines refer to the interval $k\in[\Lambda/(s_1s_2),\Lambda/s_1]$ and the dotted lines — to the interval $k\in[\Lambda/s_1,\Lambda]$. The proof consists of a straightforward checking of the corresponding diagram identity by the decomposition described at the end of Sec. 3.4. Note only that the wave vectors in the diagrams of $f(s_2)$ are rescaled by the factor $1/s_1$. As a test of consistency, we verify that (57) is a solution of (59).

As regards the parameter c, it appears as a common factor in the fixed–point equation obtained by setting $c'=c$ and $u=u^*$ in (23), taking into account that $u^*\propto c^2$, whereas the diagrams involved are proportional to $1/c^3$. Hence, if this equation is satisfied, then it holds for any c. In fact, the equation $c'=c$ reduces to one for the exponent η:

$$\eta\ln s = -\frac{2(n+2)}{(n+8)^2K_4^2}\,\widetilde{\Pi}(s)\,\varepsilon^2 + \mathcal{O}\left(\varepsilon^3\right)\ , \tag{60}$$

where

$$\widetilde{\Pi}(s) = \lim_{\zeta\to\infty}\lim_{k\to 0}\left\{k^{-2}\left[\ \mathbf{k}\ \ +3\left(\ \mathbf{k}\ \ +\ \mathbf{k}\ \ \right)\right]\Big|_{c=1}\right\} \tag{61}$$

is calculated at $d=4$ with $q\in[\Lambda/s,\Lambda]$ corresponding to the solid lines and $q\in[\Lambda,\Lambda\zeta]$ — to the dotted lines in the diagrams. The expected universality of the critical exponent η follows from the diagram identity

$$\widetilde{\Pi}(s_1) + \widetilde{\Pi}(s_2) = \widetilde{\Pi}(s_1 s_2)\ , \tag{62}$$

which implies that $\widetilde{\Pi}(s)\propto\ln s$ holds and, therefore, η is independent of s. The identity (62) is proven by the same method as (59). In principle, the critical exponent η can be calculated from (60) at any given s. However, from a technical point of view, it is convenient to consider the limit $s\to\infty$, since only the first diagram in (61) provides the singular contribution $\sim\ln s$ in this case. Hence, we have

$$\eta = -\frac{2(n+2)}{(n+8)^2K_4^2}\,\varepsilon^2\times\lim_{s\to\infty}\lim_{k\to 0}\left\{\frac{1}{k^2\ln s}\left(\ \mathbf{k}\ \ \right)\Big|_{c=1}\right\} + \mathcal{O}\left(\varepsilon^3\right)\ . \tag{63}$$

Rescaling the wave vectors by factor s/Λ, $\lim\limits_{s\to\infty}\lim\limits_{k\to 0}\{\cdot\}$ in (63) reduces to the expansion coefficient at $k^2\ln s$ in the asymptotic large–s expansion of the diagram $\mathbf{k}$, in which $q\in[1,s]$ corresponds to the dotted lines. This coefficient can be calculated from (49) at $\zeta=s$, and is equal to $-K_4^2/4$. It yields the well known result (see, e. g., [2])

$$\eta = \frac{1}{2}\frac{n+2}{(n+8)^2}\,\varepsilon^2 + \mathcal{O}\left(\varepsilon^3\right)\ . \tag{64}$$

Closing this section, we note that the independence of the fixed–point function $\theta^*(\mathbf{k})$ on the RGT scale parameter s can be easily seen when using the diagrammatic representation (28), taking into account that this diagram converges to certain s–independent value at $\zeta \to \infty$, as shown in Sec. 3.3.

4 A refined diagrammatic renormalization

Here we consider a refined renormalization scheme, taking into account the correction terms omitted in the derivations of Sec. 3.2. In this case the only approximation is that the vertices of higher than $\mathcal{O}\left(\varepsilon^2\right)$ orders are omitted.

To simplify the notation, consider first the one–component case $n = 1$, where the symbol Σ in (17) can be omitted. The dashed lines, similarly as dotted and solid coupling lines, are related to the propagator $1/(ck^2)$ in the notations used in this section.

After m RG transformations with a constant scale factor s, the terms with a_4 and a_6 in (17) now look as

$$\sum_{j,l=1}^{m} (a_4)_{jl} \Big(\quad \Big)_{jl} \ , \tag{65}$$

$$\sum_{j=1}^{m} (a_6)_{j} \Big(\quad \Big)_{j} \ , \tag{66}$$

where the indices j and l are used to distinguish between diagrams with different k intervals related to the coupling lines. Namely, the dotted lines in the diagrams refer to $k \in [\Lambda s^{j-1}, \Lambda s^{j}]$, whereas the dashed line — to $k \in [\Lambda s^{l-1}, \Lambda s^{l}]$. In the RG flow equations of Sec. 3.1 we have $(a_4)_{jl} = a_4$ and $(a_6)_j = a_6$, whereas here these weight coefficients are slightly different.

The generalisation to the n–component case is possible by using the decompositions of the kind (65) and (66) for the diagram of each topology when deciphered as one composed of the vertices instead of .

Within the $\mathcal{O}\left(\varepsilon^3\right)$ error of the actual truncation scheme, the weight coefficients $(a_4)_{jl}$ and $(a_6)_j$ after m RG transformations, i. e., $(a_4)_{jl}(m)$ and $(a_6)_j(m)$, are given by the recurrence relations

$$(a_6)_1(m) = -\frac{1}{8} R_m s^{2\varepsilon-3\eta}\, u^2(m-1) \tag{67}$$

$$(a_6)_j(m) = R_m s^{2\varepsilon-3\eta}\, (a_6)_{j-1}(m-1) \quad : \quad 2 \le j \le m\,,\ m \ge 2 \tag{68}$$

$$(a_4)_{11}(m) = -\frac{9}{16} R_m^2 s^{2\varepsilon-2\eta}\, u^2(m-1) \tag{69}$$

$$(a_4)_{1j}(m) = (a_4)_{j1}(m) = \frac{9}{2} R_m^2 s^{2\varepsilon-2\eta}\, (a_6)_{j-1}(m-1) \quad : \quad 2 \le j \le m\,,\ m \ge 2 \tag{70}$$

$$(a_4)_{jl}(m) = R_m^2 s^{2\varepsilon-2\eta}\, (a_4)_{j-1,l-1}(m-1) \quad : \quad 2 \le j \le m\,,\ 2 \le l \le m\,,\ m \ge 2 \tag{71}$$

where $R_m = c(m)/c(m-1)$ is the ratio of c values in two subsequent RG transformations. We have denoted by $u(m)$ and $c(m)$ the values of u and c, respectively, after the m–th RGT, the initial values being given by $u(0)$ and $c(0)$. Eq. (67) represents the contribution due to the coupling like and rescaling of two ordinary φ^4 vertices, whereas the coefficients (68) are the weight factors of the corresponding terms rescaled repeatedly. Eq. (69) corresponds to the coupling and rescaling of two ordinary φ^4 vertices like , whereas (70) — to the

coupling of two lines of the vertex 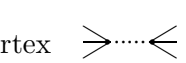 with $k \in [\Lambda s^{j-2}, \Lambda s^{j-1}]$ related to the dotted line, followed by the rescaling of the diagram. Although there are 9 combinatorial possibilities to couple these lines, the factor 9/2 in (70) is twice smaller. It is because the corresponding term appears twice in the decomposition (65), i. e., as $(a_4)_{1j}$ and $(a_4)_{j1}$. Finally, (71) comes from the rescaling of the quartic terms (69) and (70). The actual update rules (67) to (71) are consistent with the fact that the range of the wave vectors for the internal lines of any diagram is rescaled by the factor s in each RGT, taking into account the corresponding rescaling factors discussed in previous sections. Here, however, additional rescaling factors R_m and R_m^2 appear, which have been neglected before. They originate from the renormalization of parameter c: since the diagrams are defined so that factors $1/(ck^2)$ correspond to the coupling lines, these factors need to be redefined with new value of c after each RGT. Hence, the weight coefficient for a diagram with l such coupling lines gets a factor R_m^l.

Eqs. (67) to (71) can be applied also to the general n–component case. In this case $(a_4)_{jl}$ are the common factors for the weighted sum of diagrams of three different topologies appearing in (14) with the corresponding k intervals for the coupling lines. It is obviously true because the diagrams of these three topologies always appear with certain relative weight factors, which depend only on n and are the same as in (14).

Since u and c are varied only by an amount of $\mathcal{O}(\varepsilon^2)$ in one RGT, it easy to verify that Eqs. (67) to (71) provide $(a_4)_{jl}(m) = (a_4)_{11}(m) + \mathcal{O}(\varepsilon^3)$ and $(a_6)_j(m) = (a_6)_1(m) + \mathcal{O}(\varepsilon^3)$ for any m and $j \leq M$, $l \leq M$ at any large but finite M. Besides the values of these coefficients are consistent within the $\mathcal{O}(\varepsilon^3)$ error with the corresponding values of a_4 and a_6 provided by (19) and (20) after m RG transformations. Since the diagram 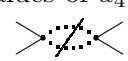 is convergent when the wave vectors within $[\Lambda, \infty]$ are related to the dotted lines (see Sec. 3.3), the contribution of infinitely large wave vectors is unimportant here. Hence, calculations here and in Sec. 3 yield consistent estimates of the renormalized Hamiltonian.

5 Renormalization up to the order of ε^3

5.1 Vertices of the order $\mathcal{O}(\varepsilon^3)$

According to our diagrammatic representation, vertices of the order $\mathcal{O}(\varepsilon^3)$ in the renormalized Hamiltonian are those made by coupling three original vertices of (2), as well as other diagrams of such topology. The following rigorous statements are used to find the topological pictures, made by coupling lines, corresponding to the vertices of the order $\mathcal{O}(\varepsilon^3)$. These are the topological pictures obtained when the dashed lines of the vertices 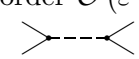 shrink to points, so that we deal with instead.

Lemma 1. *Any connected diagram made of three vertices* *contains a subset of two coupling lines connecting the nodes as in the diagram* 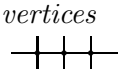 *.*

Proof. Let number the vertices as vertex 1, vertex 2, and vertex 3. Since the diagram is connected, vertex 1 must be connected at least with one line either to vertex 2 or to vertex 3, and these two connected vertices must be connected with at least one line to the remaining vertex. Hence such a subset of connecting lines as in the diagram 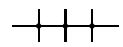 always exists. □

Lemma 2. *Any diagram of the renormalized Hamiltonian containing a subgraph (which is not the whole diagram) of topology* , , , , 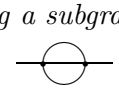 *, etc., i. e.,*

a subgraph with two outgoing lines, can be nonvanishing only if the lines of this subgraph are the internal ones of the whole diagram.

Proof. The considered subgraphs have opposite wave vectors $\mathbf{k}$ and $-\mathbf{k}$ related to their two outgoing lines, as it follows from the fact that the sum of the wave vectors entering each node in a Feynman diagram is vanishing. On the other hand, by definition of the RGT, the internal and the external lines in the diagrams of the renormalized Hamiltonian always have different values of $|\,\mathbf{k}\,|$. Hence, the diagram can be nonvanishing only if both outgoing lines of the subgraph are either internal or external lines of the whole diagram. Only the first scenario is possible, since the subgraph has to be connected to the rest of the diagram. □

Lemma 3. *Any connected diagram with at least four external lines, which is a nonvanishing diagram of the renormalized Hamiltonian and is made of two vertices* *and one vertex* *, contains a subset of two coupling lines connecting the nodes as in the graph* 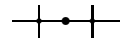 *.*

Proof. The lines of the vertex have to be the internal lines of the diagram according to *Lemma 2*. Hence, there are two possible ways how these lines can be coupled to the rest of the diagram: (1) they are connected to two lines of one of the vertices as ; and (2) they are connected to both vertices as . In the first case, the remaining vertex has to be connected as to obtain a diagram with at least four external lines. This diagram, however, is vanishing according to *Lemma 2*. Hence, only the second possibility remains, i. e., the subset of coupling lines contained in the diagram 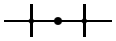 always exists. □

It is easy to verify that nonvanishing connected diagrams made of two vertices and one vertex can contain no more than two external lines. Thus, *Lemma 1* and *Lemma 3* imply that the diagrams of order $\mathcal{O}\left(\varepsilon^3\right)$ with at least four external lines can have only the following topologies: 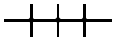 , , and those ones obtained by coupling the lines in these graphs. Using also *Lemma 2*, it allows to find easily all the nonvanishing diagrams of this type. In such a way, the renormalized Hamiltonian has the form

$$H = H^{(2)} + H^{(4)} + H^{(6)} + H^{(8)} + \mathcal{O}\left(\varepsilon^4\right) \,, \tag{72}$$

where $H^{(2m)}$ includes all the φ^{2m}–type vertices representable by the diagrams with $2m$ external lines. The corresponding algebraic representation is

$$\frac{H^{(2m)}}{T} = V^{1-m} \sum_{i_1,\ldots,i_m} \sum_{\mathbf{k}_1,\mathbf{q}_1,\ldots,\mathbf{k}_m,\mathbf{q}_m} Q_m\left(\mathbf{k}_1,\mathbf{q}_1,\ldots,\mathbf{k}_m,\mathbf{q}_m\right) \varphi_{i_1,\mathbf{k}_1}\varphi_{i_1,\mathbf{q}_1}\cdots\varphi_{i_m,\mathbf{k}_m}\varphi_{i_m,\mathbf{q}_m} \,. \tag{73}$$

In such a form $Q_m\left(\mathbf{k}_1,\mathbf{q}_1,\ldots,\mathbf{k}_m,\mathbf{q}_m\right)$ vanishes unless $\sum_i \mathbf{k}_i + \mathbf{q}_i = \mathbf{0}$. The dependence of these weight factors on various parameters is not indicated here.

As regards the quartic part $H^{(4)}$, we need to separate the contribution corresponding the ordinary φ^4 vertex, which is provided by the constant part of the weight function Q_2 in (73) evaluated at $\mathbf{k}_i = \mathbf{q}_i = \mathbf{0}$. For this purpose we can represent each diagram of $H^{(4)}$ as

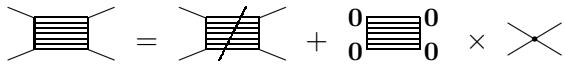

(74)

In this symbolic notation 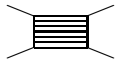 is any diagram with four external lines, whereas 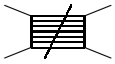 is the same diagram from which the contribution corresponding to the ordinary φ^4 vertex is subtracted. The latter one is represented by the last term in (74), where is the diagram with amputated external lines having zero wave vectors. A particular example

(75)

refers to the diagrams already considered in Sec. 3. A problem here is that not all diagrams of the kind 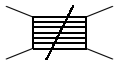 are convergent when the integration region for the internal lines $[\Lambda, \Lambda\zeta]$ is extended to infinity at $\zeta \to \infty$. To avoid possible unphysical divergence and instability of the RG flow, a suitable representation of the renormalized Hamiltonian should be used, where all vertices are convergent at $\zeta \to \infty$. It is reached by making appropriate zero–$\mathbf{k}$ subtractions not only from the entire φ^4 diagrams, but also from their internal parts, like, e. g., 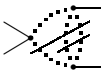 and . In the latter case, it is not necessary to make an extra subtraction of the zero–$\mathbf{k}$ contribution from the whole diagram, since such a contribution is vanishing. Appropriate subtractions should be used also for vertices of higher than φ^4 order to ensure their convergence at $\zeta \to \infty$.

5.2 The renormalized Hamiltonian and RG flow equations

According to the analysis of Sec. 5, an appropriate representation of the renormalized Hamiltonian is

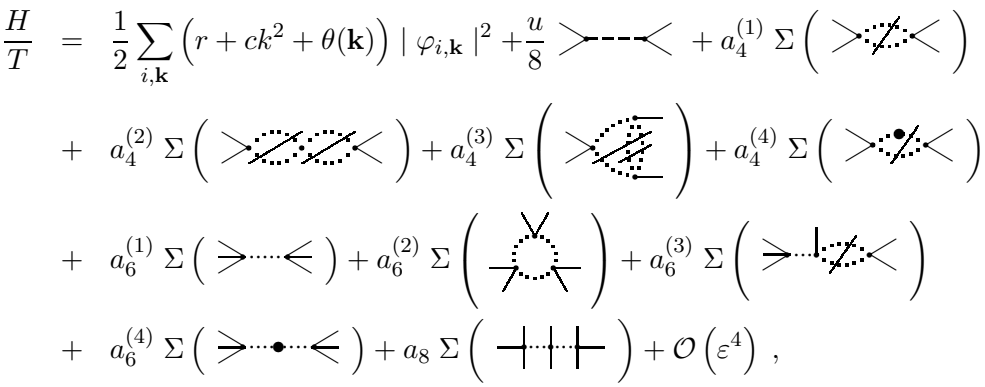

(76)

where $\Sigma(\cdot)$ denotes the sum of all such diagrams made of vertices 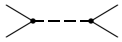 and , which yield the given picture when the dashed lines shrink to points. Besides, the combinatorial weight coefficients, including the n–dependent factors, are normalized in such a way that their sum is 1 at $n = 1$. The relations of the kind

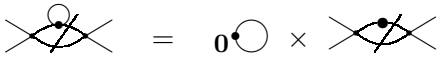

(77)

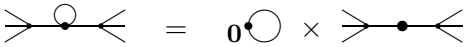

(78)

have been applied to reduce the number of different kind of vertices in the representation of the Hamiltonian. The wave vectors of dotted lines are within $k \in [\Lambda, \Lambda\zeta]$ with ζ being updated as $\zeta' = s\,\zeta$ under the RG transformation R_s.

The other Hamiltonian parameters are updated as follows:

$$
\begin{aligned}
u' &= s^{\varepsilon-2\eta}\Bigg[u - \frac{n+8}{2}u^2\ \mathbf{0}\!\!\bigcirc\!\!\!

Here $Q = \hat{Q}(s)/\ln s$, where $\hat{Q}$ is given by the diagram expression

$\hat{Q}(s) =$ 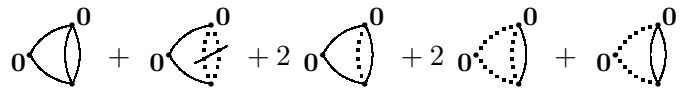 (91)

evaluated at $d = 4$ and $c = 1$. The quantity $\hat{Q}(s)$ is proportional to $\ln s$, since $\hat{Q}(s_1 s_2) = \hat{Q}(s_1) + \hat{Q}(s_2)$ holds at $\zeta \to \infty$ as a diagram identity, which can be verified by the method outlined in Sec. 3.4. Hence, Q is s–independent and, therefore, u^* is s–independent at least up to the ε^2 order, as expected. It is convenient to consider the limit $s \to \infty$ to determine Q from

$Q =$ 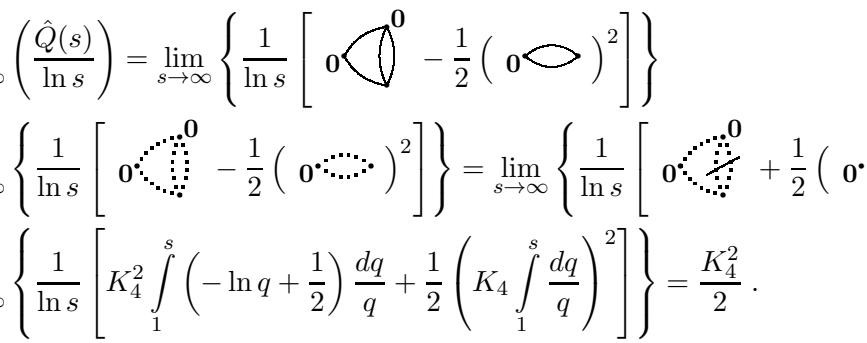

$$= \lim_{s\to\infty} \left\{ \frac{1}{\ln s} \left[K_4^2 \int_1^s \left(-\ln q + \frac{1}{2} \right) \frac{dq}{q} + \frac{1}{2} \left(K_4 \int_1^s \frac{dq}{q} \right)^2 \right] \right\} = \frac{K_4^2}{2} \,. \tag{92}$$

The wave vectors are rescaled to $k \in [1, s]$ (i. e., this interval corresponds to the dotted lines in the diagrams of (92)) and the zero–$\mathbf{k}$ contribution of the internal diagram block is separated in the second line of (92). The large–k asymptotic estimate for , obtained in Sec. 3.3, is used in the third line of (92). Inserting this result into (90), we obtain

$$a_1(n) = \frac{3(3n+14)}{(n+8)^2} \,. \tag{93}$$

Summarising the results of this section, one has to note that, at the ε^3 order, the renormalized Hamiltonian contains several extra vertices as compared to the initial or bare Hamiltonian. All these terms, including the φ^6 vertices and the φ^8 vertex, are relevant in the sense that they do not vanish at the fixed point.

6 Expansion at a fixed spatial dimension d

Apart from the ε–expansion, we have tested also an alternative approach, where the coupling constant u is considered as an expansion parameter at a fixed spatial dimensionality, i. e., fixed ε. In this sense the discussed here approach is similar in spirit to that widely used for calculations in three dimensions, $d = 3$, as described in [14, 15, 16, 17, 18]. This known approach uses the Callan–Symanzik equation instead of the Wilson's equation (3). However, if both are correct RG equations, then they should provide consistent results. Here we use (3) to make the expansion in powers of u at a fixed but small ε.

In this method, all the rescaling factors of the kind s^ε have to be retained in their original form without the expansion in powers of ε. Following the approach of [14, 15, 16, 17, 18], the critical exponents should be expanded in powers of the coupling constant, estimating their universal values at $u = u^*$. Therefore, the correction factors like $s^{-\eta}$ can be omitted in the first approximation, since one finds that $\eta = \mathcal{O}\left(u^2\right)$. Using this idea, and following the calculations

in Sec. 3.1, we determine the fixed–point values of u and r in the lowest order of the theory, i. e., $\tilde{u}^*$ and $\tilde{r}^*$, as

$$\tilde{u}^* = \frac{c^2\Lambda^\varepsilon}{K_d\, s^\varepsilon}\ \frac{2}{n+8}\ \varepsilon\ , \tag{94}$$

$$\tilde{r}^* = -\frac{s^2 - s^\varepsilon}{s^{2+\varepsilon} - s^\varepsilon}\ \frac{c\Lambda^2}{2-\varepsilon}\ \frac{n+2}{n+8}\ \varepsilon\ . \tag{95}$$

These values are obtained as the fixed–point solutions of (21) and (22), retaining the relevant terms without their expansion in powers of ε. In this case the terms up to the lowest–order diagrams, $\mathbf{0}$ in (21) and $\mathbf{0}$ in (22), have been included.

As we see, the fixed–point values depend on the scale parameter s, thus pointing to an internal inconsistency of this method. It is in contrast to the results of the ε–expansion, where such a problem was not detected.

7 The two–point correlation function

7.1 The diagrammatic representation and scaling

Consider now the Fourier–transformed two–point correlation function $G(\mathbf{k}) = \langle |\ \varphi_{i,\mathbf{k}}\ |^2 \rangle$. Its diagram expansion contains all connected diagrams with two external lines, having wave vectors $\mathbf{k}$ and $-\mathbf{k}$. Thus we have

$G(\mathbf{k}) =$ 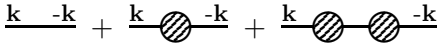 $+ \ldots = \dfrac{G_0(\mathbf{k})}{1 - 2G_0(\mathbf{k})\widetilde{\Sigma}(\mathbf{k})}\ ,$ (96)

where 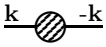 represents the sum of diagrams of this kind, which are made of vertices of $-H/T$ and are irreducible in the sense that they are not representable as a chain of such blocks. Here $\widetilde{\Sigma}(\mathbf{k}) =$ 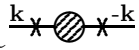 is such irreducible diagram block with amputated external lines. The quantity $-2\widetilde{\Sigma}(\mathbf{k})$ is known as self–energy [2]. The well known expansion (96) leads to the equation

$$X(\mathbf{k}) = ck^2 - 2\widetilde{\Sigma}(\mathbf{k})\ , \tag{97}$$

where $X(\mathbf{k}) = 1/G(\mathbf{k})$ is the inverse of the two–point correlation function, and $G_0(\mathbf{k})$ is set to $1/(ck^2)$ within the ε–expansion. In this case, the diagrams contain also insertions of the second–order vertex $(1/2)\sum_{i,\mathbf{k}}(r + \theta(\mathbf{k}))\ |\ \varphi_{i,\mathbf{k}}\ |^2$. The wave vectors within $q \in [0, \Lambda]$ are related to the solid coupling lines between different vertices in these diagrams. The vertices themselves can contain internal dotted lines with $q \in [\Lambda, \Lambda\zeta]$, produced by the RG transformation, ζ being the renormalization scale in the RG flow equations.

As it is well known, the two–point correlation function rescales in accordance with

$$X(\mathbf{k}; R_s H) = s^{2-\eta} X(\mathbf{k}/s; H) \tag{98}$$

after the RG transformation R_s, transforming the original Hamiltonian H into the renormalized one $R_s H$. It is a general exact relation, trivially following from the fact that the integration over the Fourier modes with $\Lambda/s < k < \Lambda$ in the first step of the RG transformation does not alter the correlation function for $k < \Lambda/s$, whereas the s–dependent factors in (98) compensate its rescaling in the second step of the RG transformation (see Sec. 2).

7.2 The two–point correlation function at the fixed point

In the following, we will examine the two–point correlation function (or its inverse) at the fixed point up to the ε^2 order. According to (98), $X(\mathbf{k}) = ak^{2-\eta}$ holds within $k \leq \Lambda$ for the fixed–point Hamiltonian H^* (since $R_s H^* = H^*$) with some $\mathbf{k}$–independent constant a, which can depend on n, ε, and Hamiltonian parameters. It is consistent with (97) if

$$ak^2(1-\eta\ln k) = ck^2 - \frac{n+2}{2}u^{*2}\Bigg\{ \mathbf{k}\,\Sigma + \mathbf{k}\,\Phi + 3\Big(\mathbf{k}\,\Phi + \mathbf{k}\,\Phi \Big)\Bigg\} + \mathcal{O}\left(\varepsilon^3\right) \qquad (99)$$

holds for $k \leq \Lambda$, since $\widetilde{\Sigma}(\mathbf{0})$ vanishes at the fixed point. Note that $q \in [0, \Lambda]$ refers to the solid lines and $q \in [\Lambda, \Lambda\zeta]$ at $\zeta \to \infty$ – to the dotted lines in (99). The diagrams can be evaluated at $d = 4$ in this case, and we can set $c = 1$, as it gives merely a common factor. By definition of $\mathbf{k}\,\Sigma$, we have

$$\mathbf{k}\,\Sigma = \mathbf{k}\,\Phi - k^2 R(\zeta)\ , \qquad (100)$$

where

$$R(\zeta) = \lim_{k\to 0}\left\{\frac{1}{k^2}\ \mathbf{k}\,\Phi\right\} = -\frac{K_4^2}{4}\ln\zeta + const \qquad \text{at} \quad d=4, \quad \zeta\to\infty\ , \qquad (101)$$

as consistent with the already considered estimation of such term (after rescaling the wave vectors from $q \in [\Lambda, \Lambda\zeta]$ to $q \in [1, \zeta]$) at the end of Sec. 3.5. Inserting (100) into (99), and summing up the diagrams, we obtain (at $c = 1$)

$$ak^2(1-\eta\ln k) = k^2 - \frac{n+2}{2}u^{*2}f(k,\zeta) + \mathcal{O}\left(\varepsilon^3\right) \qquad \text{at} \quad \zeta\to\infty\ , \qquad (102)$$

where

$$f(k,\zeta) = \mathbf{k}\,\Phi - k^2 R(\zeta) \qquad (103)$$

with $q \in [0, \Lambda\zeta]$ corresponding to the dashed lines. Using (101) and rescaling the wave vectors, we find that

$$f(k) = \lim_{\zeta\to\infty} f(k,\zeta) \qquad (104)$$

obeys the equation

$$f(sk) = s^2\left(f(k) + \frac{1}{4}K_4^2\,k^2\ln s\right) \qquad (105)$$

with the solution

$$f(k) = \mathcal{B}\,k^2 + \frac{1}{4}K_4^2\,k^2\ln k\ , \qquad (106)$$

where $\mathcal{B}$ is a constant. According to this, Eq. (102) is indeed satisfied with appropriate $a = a(n,\varepsilon)$ at η given by (64). In such a way, we have verified that the ε–expansion of $X(\mathbf{k})$ at the fixed point is consistent with the scaling $X(\mathbf{k}) = ak^{2-\eta}$ within $k \leq \Lambda$ up to the order of ε^2, at least. Besides, such analysis provides one more method to determine the critical exponent η.

7.3 The two–point correlation function on the critical surface

7.3.1 Some consistency relations

The critical correlation function diverges at $k \to 0$, so that $X(\mathbf{0}) = 0$ and $\widetilde{\Sigma}(\mathbf{0}) = 0$ must hold in this case, which means that (97) becomes

$$X(\mathbf{k}) = ck^2 - 2[\widetilde{\Sigma}(\mathbf{k}) - \widetilde{\Sigma}(\mathbf{0})] \; . \tag{107}$$

It is easy to verify that the condition $\widetilde{\Sigma}(\mathbf{0}) = 0$ is indeed satisfied in the lowest order of the ε–expansion, where the equation of the critical surface reads

$$r = r_c(u) = -\frac{n+2}{2} u \; \mathbf{0} \bullet\!\!\bigcirc \; + \mathcal{O}\left(\varepsilon^2\right) \tag{108}$$

with $k \in [0, \Lambda]$ for the solid lines. The condition $\widetilde{\Sigma}(\mathbf{0}) = 0$ should hold on the critical surface also at higher orders of the ε–expansion. We have tested this expected property up to the ε^3 order and have not revealed any contradiction.

According to (107), the equation for $X(\mathbf{k})$ on the critical surface reads

$$X(\mathbf{k}) = ck^2 - \frac{n+2}{2} u^2 \Bigg\{ \mathbf{k} \; + \; \mathbf{k} \; + 3 \Bigg(\mathbf{k} \; + \; \mathbf{k} \; \Bigg) \Bigg\} + \mathcal{O}\left(\varepsilon^3\right) \; . \tag{109}$$

Based on this equation, we will consider the rescaling of $X(\mathbf{k})$ in the renormalization process, starting with the bare Hamiltonian at $(u - u^*)/u^* = \delta_0$ and $c = c_0$ and performing certain number m of RG transformation R_s, in such a way that $(u - u^*)/u^*$ becomes equal to δ, where δ_0 and δ are small constants. In this case, the fixed–point value u^* of the coupling constant is determined at the current value of the parameter c, so that it is a slightly varying quantity due to the renormalization of c. Such a choice is convenient, since we do not need to determine the fixed–point value of c after infinite number of RG transformations. In the actually considered truncation of the ε–expansion, the renormalization of u is given by (21), from which we evaluate $m = m(\delta_0, \delta, s, \varepsilon)$. In this case, $m \sim 1/\varepsilon$ is determined with uncertainty of $\mathcal{O}(1)$, so that it can be rounded to appropriate integer value at any positive $s - 1$ of order unity. The renormalization of $(u - u^*)/u^*$ can be performed at integer m for ε–independent δ_0 and δ up to any higher order of the ε–expansion by adjusting s as $s = s_0 + s_1\varepsilon + s_2\varepsilon^2 + \cdots$. The entire renormalized Hamiltonian after $m \sim 1/\varepsilon$ RGT is well defined within the ε–expansion, since we always can reach the required accuracy, truncating the RG flow equations at high enough order.

Our aim is to compare the perturbative rescaling of $X(\mathbf{k})$ with the exact one (98) at $k \to 0$, taking into account the expected asymptotic form of $X(\mathbf{k})$ on the critical surface. Namely, for the initial Hamiltonian we have

$$X(\mathbf{k}; H_0) = A(\delta_0, \varepsilon)\, k^{2-\eta} \left\{ 1 + \sum_i a_i(\delta_0, \varepsilon) k^{\omega_i} + \sum_i \hat{a}_i(\delta_0, \varepsilon) k^{\hat{\omega}_i} \right\} \qquad \text{at} \quad k \to 0 \; , \tag{110}$$

where the argument H_0 means the initial Hamiltonian, ω_i are those correction–to–scaling exponents, which tend to zero at $\varepsilon \to 0$, whereas $\hat{\omega}_i$ are those ones, which tend to positive constants in this limit. Eq. (98) then yields

$$X(\mathbf{k}; R_{s^m} H_0) = A(\delta_0, \varepsilon)\, k^{2-\eta} \left\{ 1 + \sum_i a_i(\delta_0, \varepsilon) s^{-m\omega_i} k^{\omega_i} + \sum_i \hat{a}_i(\delta_0, \varepsilon) s^{-m\hat{\omega}_i} k^{\hat{\omega}_i} \right\} \quad \text{at} \quad k \to 0 \; , \tag{111}$$

where $R_{s^m} H_0$ denotes the renormalized Hamiltonian after m RG transformations R_s. The well known result of the ε–expansion states that the leading correction–to–scaling exponent is

$$\omega := \omega_1 = \varepsilon + \mathcal{O}\left(\varepsilon^2\right) \ . \tag{112}$$

In the following, we will formulate as a theorem an important result, stating certain consistency relations for the coefficients and exponents in (110).

Theorem. *If the perturbative ε–expansion–based renormalization (repeating the RG transformation R_s) of $X(\mathbf{k}) = 1/G(\mathbf{k})$ on the critical surface is consistent with (110) and (111) at any small ε–independent δ_0 and δ, such that $0 < \delta/\delta_0 < 1$, defining the initial (δ_0) and the final (δ) value of $(u - u^*)/u^*$ (with u^* determined at the current c), then*

$$\omega_j = j\,\varepsilon + \mathcal{O}\left(\varepsilon^2\right) \qquad : \qquad j \geq 1 \ , \tag{113}$$

$$A(\delta_0, \varepsilon) = c_0 + \mathcal{O}(\varepsilon) \ , \tag{114}$$

$$a_j(\delta_0, \varepsilon) = b_j\,\varepsilon \left(\frac{\delta_0}{1+\delta_0}\right)^j + \mathcal{O}\left(\varepsilon^2\right) \qquad : \qquad j \geq 1 \tag{115}$$

hold, where c_0 is the initial value of c, and the coefficients b_j are found from the equation

$$-\eta + \varepsilon^2 \sum_{j\geq 1} j\, b_j \left(\frac{\delta}{1+\delta}\right)^j = -\eta\,(1+\delta)^2 + \mathcal{O}\left(\varepsilon^3\right) \ , \tag{116}$$

requiring the consistency of both sides at each power of δ in the small–δ–expansion.

Proof. Let us first determine the number $m = m(\delta_0, \delta, s, \varepsilon)$ of RGT required for transformation of $(u - u^*)/u^*$ from δ_0 to δ. From (21) we obtain the updating rule for $\delta_\ell = (u_\ell - u^*_\ell)/u^*_\ell$,

$$\frac{\delta_{\ell+1}}{\delta_\ell} = s^{-\varepsilon(1+\delta_\ell)+\mathcal{O}\left(\varepsilon^2\right)} \ , \tag{117}$$

where u_ℓ is the value of u after ℓ-th RGT, and $u^*_\ell = u^*(c_\ell)$ is the fixed–point value of u determined at the current c after ℓ-th RGT, i. e., at $c = c_\ell$. Here we take into account that $c_{\ell+1} = c_\ell + \mathcal{O}\left(\varepsilon^2\right)$ holds according to (23) and therefore $u^*_{\ell+1} = u^*_\ell + \mathcal{O}\left(\varepsilon^3\right)$ follows from (89). Denoting $x_\ell = \ln \mid \delta_\ell \mid$, Eq. (117) reduces to

$$x_{\ell+1} - x_\ell = -\varepsilon\ \left(1 + \mathrm{sign}(\delta)\, e^{x_\ell}\right) \ln s + \mathcal{O}\left(\varepsilon^2\right) \ . \tag{118}$$

The variation of x_ℓ becomes quasi–continuous in the limit $\varepsilon \to 0$, so that x_ℓ can be considered as a continuous function $x(\ell)$, and (118) transforms into the differential equation

$$\frac{dx(\ell)}{d\ell} = -\varepsilon\,\left(1 + \mathrm{sign}(\delta)\, e^x\right) \ln s + \mathcal{O}\left(\varepsilon^2\right) \ . \tag{119}$$

Integrating this equation, we find the necessary number of RGT

$$m = \frac{1}{\varepsilon \ln s} \int\limits_{x_*}^{x_0} \frac{dx}{1 + \mathrm{sign}(\delta)\, e^x} + \mathcal{O}(1) = \frac{1}{\varepsilon \ln s} \ln\left[\frac{\delta_0(1+\delta)}{(1+\delta_0)\delta}\right] + \mathcal{O}(1) \ , \tag{120}$$

where $x_0 = \ln \mid \delta_0 \mid$ is the initial and $x_* = \ln \mid \delta \mid$ is the final value of $\ln \mid \delta_\ell \mid$. It yields

$$s^{-m\varepsilon} = \frac{1+\delta_0}{\delta_0} \times \frac{\delta}{1+\delta} + \mathcal{O}(\varepsilon) \ . \tag{121}$$

Inserting (121) into (111), we obtain

$$X(\mathbf{k}; R_{s^m} H_0) = A(\delta_0, \varepsilon)\, k^{2-\eta} \left\{ 1 + \sum_i a_i(\delta_0, \varepsilon) \left[\frac{\delta(1+\delta_0)}{(1+\delta)\delta_0} + \mathcal{O}(\varepsilon) \right]^{\omega_i/\varepsilon} k^{\omega_i} + \mathcal{O}\left(e^{-\lambda/\varepsilon} k^{\hat{\omega}} \right) \right\} , \tag{122}$$

where the terms with $\hat{\omega}_i$ are absorbed in the last remainder term, where $\lambda > 0$ and $\hat{\omega}$ is the smallest exponent among $\hat{\omega}_i$. This term is irrelevant in the ε–expansion.

From (107) we obtain

$$X(\mathbf{k}; R_{s^m} H_0) = ck^2 - \frac{n+2}{2c^3} \left[u^*(1+\delta) \right]^2 \left(\mathcal{B}\, k^2 + \frac{1}{4} K_4^2\, k^2 \ln k \right) + \mathcal{O}\left(\varepsilon^3 \right) . \tag{123}$$

The diagrams of (107) are evaluated in (123) as in Sec. 7.2 (cf. Eq. (106)), since the difference between the cases $\zeta = \infty$ and $\zeta = s^{m(\delta_0, \delta, s, \varepsilon)}$ (with $q \in [\Lambda, \Lambda\zeta]$ for dotted lines) is irrelevant within the ε–expansion. Since c is renormalized by $\mathcal{O}\left(\varepsilon^2\right)$ in one RGT according to (23), the renormalized c value after $m \sim 1/\varepsilon$ RG transformations in (123) is $c = c_0 + \mathcal{O}(\varepsilon)$.

The consistency with (122) (where $\omega_i \to 0$ at $\varepsilon \to 0$) implies that $X(\mathbf{k}; R_{s^m} H_0)$ can be expanded as

$$X(\mathbf{k}; R_{s^m} H_0) = k^2 \left(\mathcal{B}_0(\delta_0, \delta, \varepsilon) + \mathcal{B}_1(\delta_0, \delta, \varepsilon) \ln k + \mathcal{B}_2(\delta_0, \delta, \varepsilon) (\ln k)^2 + \cdots \right) \tag{124}$$

at $\varepsilon \to 0$. On the other hand, the diagrammatic perturbative equation for $X(\mathbf{k}; R_{s^m} H_0)$ on the critical surface can be represented in general (up to any order of the ε–expansion) as

$$X(\mathbf{k}; R_{s^m} H_0) = c\, F(\mathbf{k}, \delta, \varepsilon) , \tag{125}$$

where $c = c(\delta_0, \delta, \varepsilon)$, whereas $F(\mathbf{k}, \delta, \varepsilon)$ contains only integer powers of δ in the small–δ–expansion. It is because the critical value of r, as well as all Hamiltonian parameters can be expanded in integer powers of $u = u^*(1+\delta)$, where $u^* = u^*(c) = c^2 u^*(1)$ holds with δ_0– and δ–independent $u^*(1)$, and the diagrams associated with u^ℓ contain $2\ell - 1$ internal coupling lines giving the factor $c^{1-2\ell}$. These are consequences of the general structure of the RG flow equations. Hence, the small–δ–expansion of the ratio $\mathcal{B}_i(\delta_0, \delta, \varepsilon)/\mathcal{B}_0(\delta_0, \delta, \varepsilon)$ in (124) contains only integer powers of δ for any $i \geq 1$. Assuming that $\omega_j = d_j\, \varepsilon + \mathcal{O}\left(\varepsilon^2\right)$ holds with noninteger positive d_j for some j, we arrive at a contradiction, since then the ε–expansion in (122) produces $\mathcal{B}_i(\delta_0, \delta, \varepsilon)/\mathcal{B}_0(\delta_0, \delta, \varepsilon)$ containing noninteger powers of δ. The contradiction is obtained also if we assume the existence of ω_j of a higher order than $\mathcal{O}(\varepsilon)$, since the ε–expansion of $\mathcal{B}_i(\delta_0, \delta, \varepsilon)/\mathcal{B}_0(\delta_0, \delta, \varepsilon)$ in (122) produces powers of $\ln \delta$ in this case. We can consider also a possibility that $\omega_j \sim \varepsilon^{\mu_j}$ with noninteger μ_j holds for some indices j. It does not lead to the consistency, since the expansion of $F(\mathbf{k}, \delta, \varepsilon)$ contains only integer powers of ε, coming from the ε–expansion of u^* and diagrams evaluated at $c = 1$. In such away, (122) can be consistent with the diagrammatic perturbative equation only if (112) and (113) hold.

$X(\mathbf{k}; R_{s^m} H_0) = ck^2 + \mathcal{O}\left(\varepsilon^2\right) = c_0 k^2 + \mathcal{O}(\varepsilon)$ holds according to (123). Besides, the coefficient at $\ln k$ in (123) is of order $\mathcal{O}\left(\varepsilon^2\right)$, and it is independent of δ_0 at this order. Eqs. (114) and (115) must hold to satisfy these relations in (122), performing the ε–expansion. Finally, (116) states the necessary consistency relation for the coefficient at $\varepsilon^2 \ln k$ in (122) and (123), taking into account that $[(n+2)/(8c^3)] K_4^2 u^{*2} = c\, \eta + \mathcal{O}\left(\varepsilon^3\right)$ holds according to (55) and (64). $\square$

7.3.2 A further test of consistency

Based on the relations stated in the above theorem, here we perform some test for single RG transformation R_s on the critical surface, starting with small $(u-u^*)/u^* = \delta_0$, defined as before.

We consider the asymptotic small–$\mathbf{k}$ estimate of the inverse correlation function defined as

$$X^{as}(\mathbf{k}; H_0) := A(\delta_0, \varepsilon)\, k^{2-\eta} \left\{ 1 + \sum_i a_i(\delta_0, \varepsilon) k^{\omega_i} \right\} \tag{126}$$

obtained by neglecting the irrelevant (at $k \to 0$) terms with exponents $\hat{\omega}_i$ in (110). Following (98), it rescales exactly as

$$X^{as}(\mathbf{k}; R_s H_0) = A(\delta_0, \varepsilon)\, k^{2-\eta} \left\{ 1 + \sum_i a_i(\delta_0, \varepsilon) s^{-\omega_i} k^{\omega_i} \right\} \tag{127}$$

after the RG transformation R_s. According to (115), we can write

$$a_i(\delta_0, \varepsilon) = b_i\, \varepsilon \left(\frac{\delta_0}{1+\delta_0} \right)^i + \mathcal{E}_i(\delta_0)\, \varepsilon^2 + \mathcal{O}\left(\varepsilon^3\right) \qquad : \qquad i \geq 1 \ , \tag{128}$$

where $\mathcal{E}_i(\delta_0)$ are some unknown coefficients. Further on, we consider the expansion up to the ε^2 order for the ratio $X^{as}(\mathbf{k}; R_s H_0)/X^{as}(\mathbf{k}; H_0)$, in which case these unknown terms cancel, i. e.,

$$\frac{X^{as}(\mathbf{k}; R_s H_0)}{X^{as}(\mathbf{k}; H_0)} = 1 - \varepsilon^2 \ln s \sum_i i\, b_i \left(\frac{\delta_0}{1+\delta_0} \right)^i + \mathcal{O}\left(\varepsilon^3\right) = 1 + \eta \ln s \left[(1+\delta_0)^2 - 1 \right] + \mathcal{O}\left(\varepsilon^3\right) \ . \tag{129}$$

The sum over i in (129) is meaningful at least as the small–$[\delta_0/(1+\delta_0)]$ expansion, which gives the stated here final result after re-expanding in powers of δ_0 in accordance with (116). Thus, this is the result which holds in all orders of the small–δ_0 expansion.

In the following, we calculate the ratio $X^{as}(\mathbf{k}; R_s H_0)/X^{as}(\mathbf{k}; H_0)$ from the diagram equation (107) and compare the results. In this case we need to include those terms, which correspond to $X^{as}(\mathbf{k}; R_s H_0)$ and $X^{as}(\mathbf{k}; H_0)$ in the ε–expansion. Thus, the terms containing $k^2(\ln k)^\ell$ with $\ell \geq 0$ must be included, whereas those containing $k^\mu(\ln k)^\ell$ with $\mu > 2$ have to be neglected. Any quantity endowed with superscript "*as*" is calculated in this way. Furthermore, both $X^{as}(\mathbf{k}; R_s H_0)$ and $X^{as}(\mathbf{k}; H_0)$ are proportional to the initial c value c_0, so that we can calculate their ratio at $c_0 = 1$ without loss of generality. By definition, the term $\theta(\mathbf{k})$, represented by , tends to zero faster than $\sim k^2$ at $k \to 0$, and therefore is neglected. Thus, the diagram equation at $c_0 = 1$ yields

$$X^{as}(\mathbf{k}; H_0) = k^2 - \frac{n+2}{2} u^{*2} (1+\delta_0)^2 \Big(\mathbf{k} \Big)^{as} + \mathcal{O}\left(\varepsilon^3\right) \tag{130}$$

$$X^{as}(\mathbf{k}; R_s H_0) = ck^2 - \frac{n+2}{2} u^{*2} (1+\delta_0)^2 \Big[\Big(\mathbf{k} \Big)^{as} + 3 \Big\{ \Big(\mathbf{k} \Big)^{as} + \Big(\mathbf{k} \Big)^{as} \Big\} \Big] + \mathcal{O}\left(\varepsilon^3\right) \ , \tag{131}$$

where $q \in [0, \Lambda]$ holds for the solid lines and $q \in [\Lambda, \Lambda s]$ – for the dotted lines. Here we have set $u = u^*(1+\delta_0)$ in both expressions, since u^2 after the RGT is varied only by $\mathcal{O}\left(\varepsilon^3\right)$. The

quantity $\Big($ $\Big)^{as}$ cancels in $X^{as}(\mathbf{k}; R_s H_0)/X^{as}(\mathbf{k}; H_0)$, calculated up to the ε^2 order. The asymptotic estimate for the sum of two other diagrams at $d = 4$ and $c = 1$ is

$\Big($ $\Big)^{as}$ + $\Big($ 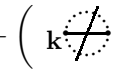 $\Big)^{as}$ $= k^2 \Phi(0, s)$, (132)

where

$\Phi(\Lambda_1, \Lambda_2) := \lim_{k\to 0} \Big\{ \frac{1}{k^2} \Big($ + 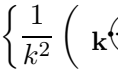 $\Big) \Big\} \Big|_{d=4}$ (133)

with $q \in [\Lambda_1, 1]$ for the solid lines and $q \in [1, \Lambda_2]$ for the dotted lines. Eq. (132) is obtained by normalizing the wave vectors ($q \to q/\Lambda$) and extracting the relevant (at $k \to 0$) contribution $\propto k^2$, neglecting corrections like $\sim k^4$, $\sim k^6$, etc. The renormalized c in (131), calculated from (23), is

$c = 1 - \eta \ln s - \frac{n+2}{2} u^{*2} (1 + \delta_0)^2 \lim_{k\to 0} \Big\{ \frac{1}{k^2} \Big($ $\Big) \Big\} \Big|_{d=4} + \mathcal{O}\left(\varepsilon^3\right)$ (134)

with $q \in [\Lambda/s, \Lambda]$ corresponding to the solid lines in the diagram evaluated at $c = 1$. If this diagram is completed by $3 \Big($ + 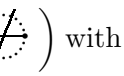 $\Big)$ with $q \in [\Lambda/s, \Lambda]$ for the solid lines and $q \in [\Lambda, \infty]$ for the dotted lines, then the obtained expression $\lim_{k\to 0} \left\{ \frac{1}{k^2} (\cdot) \right\} \Big|_{d=4}$ is exactly $\propto \ln s$, as it follows from the diagram identity (62). The proportionality coefficient is $-K_4^2/4$, in accordance with the calculations at $s \to \infty$ in Sec. 3.5. Hence, rescaling the wave vectors, we can write

$\lim_{k\to 0} \Big\{ \frac{1}{k^2} \Big($ $\Big) \Big\} \Big|_{d=4} = -\frac{K_4^2}{4} \ln s - 3\Phi(1/s, \infty)$ (135)

with $\Phi(1/s, \infty)$ defined by (133). Summarizing all the derived here diagrammatic relations for $X^{as}(\mathbf{k}; R_s H_0)$ and $X^{as}(\mathbf{k}; H_0)$, and also $[(n+2)/(8c^3)] K_4^2 u^{*2} = c\,\eta + \mathcal{O}\left(\varepsilon^3\right)$, we finally obtain

$$\frac{X^{as}(\mathbf{k}; R_s H_0)}{X^{as}(\mathbf{k}; H_0)} = 1 + \eta \left\{ \left[(1+\delta_0)^2 - 1 \right] \ln s - \frac{12}{K_4^2} (1+\delta_0)^2 \Big(\Phi(0, s) - \Phi(1/s, \infty) \Big) \right\} + \mathcal{O}\left(\varepsilon^3\right) . \tag{136}$$

It is evident that (129) and (136) agree with each other if and only if

$$\phi(s) = \Phi(0, s) - \Phi(1/s, \infty) \equiv 0 \tag{137}$$

holds for $s > 1$.

Consider now the vicinity of $s = 2$. It is a special point for one diagram of $\phi(s)$, i. e., with $q \in [0, 1]$ for the solid lines and $q \in [1, s]$ for the dotted line. Some singularity is expected here, because the integration over the region with $q > 2$ for the dotted line gives vanishing result at $k \to 0$ and, therefore, the contribution of the mentioned diagram becomes s–independent at $s = 2$, when s is increased. By definition, this contribution is equal to $\hat{\phi}(1, s)$, where

$\hat{\phi}(\Lambda_1, \Lambda_2) := \lim_{k\to 0} \Big\{ \frac{1}{k^2} \Big($ $\Big) \Big\} \Big|_{d=4}$ (138)

with $q \in [0, 1]$ corresponding to the solid lines and $q \in [\Lambda_1, \Lambda_2]$ – to the dotted line. Using the diagram identity

$$\hat{\phi}(1, \infty) = \hat{\phi}(1, s) + \hat{\phi}(s, \infty) , \tag{139}$$

we will evaluate the singular part of $\hat{\phi}(1,s)$ by calculating

$$\hat{\phi}(s,\infty) = \lim_{k\to 0}\left\{\frac{1}{k^2}\frac{1}{(2\pi)^4}\int\limits_{q<1}[\hat{I}(\mid \mathbf{q}+\mathbf{k}\mid) - \hat{I}(q)]q^{-2}d^4q\right\}\ , \tag{140}$$

where

$$\begin{aligned}\hat{I}(q) &= \quad \mathbf{q} \quad = \frac{1}{(2\pi)^4}\int\limits_{k>s} k^{-2}\mid \mathbf{q}+\mathbf{k}\mid^{-2}\Theta\left(1-\mid \mathbf{q}+\mathbf{k}\mid^2\right)d^4k \\ &= \frac{2K_4}{\pi}\int\limits_s^\infty kdk\int\limits_0^\pi \frac{\Theta\left(1-q^2-2qk\cos\theta-k^2\right)}{q^2+2qk\cos\theta+k^2}\sin^2\theta d\theta\ . \end{aligned}\tag{141}$$

Here $k\in[0,1]$ corresponds to the solid line and $k\in[s,\infty]$ – to the dotted line in the diagram. For $1<s<2$, we obtain $\hat{I}(q)=0$ if $q\le s-1$, and

$$\hat{I}(q) = \frac{2K_4}{\pi}\int\limits_s^{q+1} kdk\int\limits_{\hat{\theta}(q,k)}^{\pi}\frac{\sin^2\theta d\theta}{q^2+2qk\cos\theta+k^2} \tag{142}$$

with $\hat{\theta}(q,k)=\arccos\left[(1-q^2-k^2)/(2qk)\right]$ if $s-1<q<2$.

In the following we use the small–$\mathbf{k}$ expansion

$$\hat{I}(\mid \mathbf{q}+\mathbf{k}\mid) = \hat{I}(q) + \frac{d\hat{I}}{dq}\left(k\cos\theta+\frac{k^2}{2q}\sin^2\theta\right) + \frac{1}{2}\frac{d^2\hat{I}}{dq^2}k^2\cos^2\theta + \mathcal{O}\left(k^3\right)\ , \tag{143}$$

where θ is the angle made by $\mathbf{q}$ and $\mathbf{k}$. Inserting this into (140), we obtain

$$\hat{\phi}(s,\infty) = \frac{K_4}{8}\left(2\hat{I}(1) + (d\hat{I}/dq)\Big|_{q=1}\right) \tag{144}$$

for $1<s<2$, taking into account that $\hat{I}(q)$ and $d\hat{I}(q)/dq$ vanish at $q\le s-1$. Using (142), we find that the leading singularity

$$\hat{\phi}(s,\infty) \simeq \frac{K_4^2}{6\pi}\Delta^{3/2} \qquad \text{at} \qquad \Delta = 2-s\to 0 \tag{145}$$

is provided by the derivative term. According to (139), $-\hat{\phi}(1,s)$ has exactly such singular part. Furthermore, since $s=2$ is not any special or singular point for the diagrams of $\phi(s)$ in (137), except only the one related to $\hat{\phi}(1,s)$, we conclude that $\phi(s)$ has the same singularity as $\hat{\phi}(1,s)$. Hence, $\phi(s)\equiv 0$ cannot hold, and the consistency condition (137) is not satisfied.

This fundamental contradiction implies that the perturbative ε–expansion–based renormalization of $X(\mathbf{k})$ on the critical surface is not fully consistent with the one produced by the exact rescaling (98) of the expected asymptotic expansion (110) at small k. Note that the renormalization considered in Sec. 7.3.1 is an infinite–scale ($m\to\infty$) renormalization at $\varepsilon\to 0$. If the ε–expansion works correctly there, then it turns out that an inconsistency appears on a finite renormalization scale considered in this section. The obtained here contradiction shows that the ε–expansion fails to give correct results in the actual test, despite of the fact that it is formally well defined and stable. One has to note that the contradiction, apparently, is not caused by the violation of the rescaling rule (98) in the ε–expansion, but rather by the inconsistency with the asymptotic expansion (110), rescaled according to (98). Indeed, we have not obtained any contradiction by testing the consistency with (98) alone.

7.4 The two–point correlation function above the critical point

Consider now the inverse of the two–point correlation function above the critical point. It implies that $X(\mathbf{k})$ has to be positively defined for all $\mathbf{k}$ when the diagrams are represented by $\mathbf{k}$–space integrals. A problem here is such that the equation contains divergent diagrams. This difficulty can be overcome in a modified model where the lower cutoff $\bar{\Lambda}$ of the wave vectors is introduced. In this case $q \in [\bar{\Lambda}, \Lambda]$ corresponds to the solid coupling lines in Eq. (97), and the ε–expansion is well defined for $0 < \bar{\Lambda} < \Lambda$. Namely, we have

$$X(\mathbf{k}) = ck^2 - \frac{n+2}{2}u^2 \Big\{ \mathbf{k} \; + \; \mathbf{k} \; + 3 \Big(\mathbf{k} \; + \; \mathbf{k} \; \Big) \Big\} + \Big(r + \frac{n+2}{2} u \; \mathbf{0} \; \Big) \Big(1 - \frac{n+2}{2} u \; \mathbf{0} \; \Big) + \mathcal{O}\left(\varepsilon^3\right) \tag{146}$$

with $q \in [\Lambda, \Lambda\zeta]$ for the dotted lines at the given renormalization scale ζ. Here $\zeta = 1$ corresponds to the bare Hamiltonian. Note, however, that $\bar{\Lambda}$ is not constant, but is updated in the RG transformation R_s as $\bar{\Lambda}' = s\bar{\Lambda}$, so that $\bar{\Lambda} = \bar{\Lambda}_0\zeta$ holds, where $\bar{\Lambda}_0$ is the initial value of $\bar{\Lambda}$. Hence, it is meaningful to consider the renormalization scales $1 \leq \zeta < \Lambda/\bar{\Lambda}_0$. We have verified that the rescaling property (98) is satisfied up to the ε^2 order in this model with $r = \mathcal{O}(\varepsilon)$ and $u = \mathcal{O}(\varepsilon)$. On the other hand, we obtain certain paradox: the diagram $\mathbf{0}$ diverges and, therefore, the ε–expansion becomes unstable at $\bar{\Lambda}_0 \to 0$ despite of the fact that the correlation function in the high–temperature phase should not be singular even at $\bar{\Lambda}_0 = 0$. A standard idea, widely applied in the perturbative renormalization, is to subtract divergent terms. One believes that a physically correct result is obtained by such a method, also called renormalization. In the modified model, however, all terms are finite, i. e., there is no reason to subtract any of them at finite values of $\bar{\Lambda}_0$. Another question is whether a correct result is obtained in the original model with $\bar{\Lambda}_0 = 0$, if the divergent diagram $\mathbf{0}$ is simply discarded. The answer is negative. Indeed, it can be easily checked that $X(\mathbf{k})$ obtained in this way is inconsistent with the exact rescaling relation (98). The latter finding is not surprising: in the diagrammatic perturbation theory this relation, similarly as the semigroup property and the s–independence of the fixed point of the RG transformation R_s, is a consequence of certain diagram rescaling and summation rules. These rules cannot work to give the expected result if some diagram is simply omitted.

8 Discussion

There are a lot of perturbative RG studies of the φ^4 model made in the past (see [2, 3, 4, 19] for a review). They can be classified as approximative treatments of the perturbation theory in view of our analysis, since a set of apparently irrelevant terms is neglected. Although a perturbative RG approach to critical phenomena never could be considered as a rigorous method, it is, nevertheless, possible to calculate exactly the perturbation terms and to take them into account in a systematic way. In particular, we find that there are many different terms to be included in the renormalized Hamiltonian up to the order of ε^3, and these terms are relevant in the sense that they do not vanish when repeating the RG transformation unlimitedly many ($m \to \infty$) times. To the contrary, one usually finds that only few terms, i. e., those included already in the initial Hamiltonian (2) are relevant. A confusion about this might be caused by the fact that in the usual (nonrigorous) treatments one looks for the behaviour of individual terms and finds that most of them are shrinking in the renormalization procedure. It, however, is not a

rigorous and even not a valid argument, since the $H^{(2m)}$ parts of (72) (as well as any part of $H^{(2m)}$ represented as a sum over diagrams of certain topology) result from many such individual terms, summing up to yield relevant contributions.

The results of perturbative calculations up to the order of ε^5 are reported in literature. These, however, are based on the Callan–Symanzik equation, but not on the Wilson's equation (3). The Callan–Symanzik equation, in fact, represents a scaling property for the Hamiltonian of the form (2). The approach, thus, relies on the assumption that all the relevant terms are included in the initial Hamiltonian, only the existing here coupling constants being renormalized. This assumption is not supported by our analysis: the perturbative renormalization based on first principles (i. e., avoiding such assumptions via using (3)) produces additional relevant terms.

One believes that the ε–expansion, combined with the perturbative RG transformation, is able to describe correctly the small–$\mathbf{k}$ asymptotic of the correlation functions and the related critical phenomena. The contradiction derived in Sec. 7.3.2 causes serious doubts about it. Due to the formal character of the ε–expansion, one might happen that it describes the behaviour within any fixed range of wave vectors at $\varepsilon \to 0$ rather than the $k \to 0$ limit at a small, but fixed ε. Indeed, the contradiction might be caused by the fact that the non–Gaussian part of the Hamiltonian cannot be considered as a small perturbation, like in the ε–expansion, if one considers just the small–$\mathbf{k}$ contribution responsible for the critical fluctuations, since the Fourier amplitudes of the relevant $\varphi_i(\mathbf{x})$ configurations diverge when $k \to 0$ at criticality.

The problems and paradox discussed in Sec. 7.4 rise a question concerning that how the two–point correlation function slightly above the critical point can be correctly calculated within the ε–expansion, and whether a correct calculation method does exist here. In particular, it turns out that a simple discarding of divergent diagrams is not a correct approach, since it leads to the violation of the rescaling rule (98). In fact, certain method of calculation of the two–point correlation function has been considered in [12], where the discussed here paradox does not appear. It, however, is not based on the ε–expansion, but on certain grouping of diagrams, in such a way that the true correlation function instead of the Gaussian one is related to the coupling lines. It naturally ensures the convergence of the diagrams of the reorganized perturbation theory and allows an analytic continuation of the obtained self consistent equations from the region $r > 0$ to the vicinity of the critical point.

9 Conclusions

1. A diagrammatic formulation of the perturbative renormalization has been provided (Sec. 2), which makes calculations of perturbation terms straightforward and transparent, avoiding any intermediate approximations.

2. The RG flow equations, including all terms up to the order of ε^2, have been considered in Secs. 3 and 4. The tests of the expected properties, such as the semigroup property and the existence of an independent of the scale parameter s fixed point, have been performed. These properties are satisfied up to this order of the ε–expansion. No inconsistency has been found at the ε^3 order, as well (Sec. 5). However, some internal inconsistency has been detected in an alternative approach, where ε is fixed and the coupling constant u is an expansion parameter (Sec. 6).

3. At the ε^3 order, the renormalized Hamiltonian contains several extra (φ^4, φ^6, φ^8) vertices, as compared to the bare Hamiltonian. All these terms are relevant in the sense that they

do not vanish at the fixed point.

4. The two–point correlation function has been considered in Sec. 7 within the ε–expansion up to the order of ε^2. It is consistent with the expected power–like behaviour at the fixed point (Sec. 7.2). Nevertheless, a fundamental contradiction with the exact rescaling of the small–$\mathbf{k}$ asymptotic expansion on the critical surface exists (Secs. 7.3, 7.3.2).

5. Problems and certain paradox, related to the ε–expansion of the inverse correlation function slightly above the critical point, have been considered in Sec. 7.4.

Concerning the last three points, several related issues have been discussed in Sec. 8.

References

[1] K. G. Wilson, M. E. Fisher, Phys. Rev. Lett. **28**, 240 (1972)

[2] Shang–Keng Ma, Modern Theory of Critical Phenomena, W.A. Benjamin, Inc., New York, 1976

[3] J. Zinn–Justin, Quantum Field Theory and Critical Phenomena, Clarendon Press, Oxford, 1996

[4] H. Kleinert, V. Schulte–Frohlinde, Critical properties of ϕ^4 theories, World Scientific (2001)

[5] C. G. Callan, Phys. Rev. D **2**, 1541 (1970)

[6] K. Symanzik, Commun. math. Phys. **18**, 227 (1970)

[7] K. Symanzik, Commun. math. Phys. **23**, 49 (1971)

[8] B. Delamotte, Am. J. Phys. **72**, 170 (2004)

[9] D. Brydges, J. Dimock, T. R. Hurd, Commun. Math. Phys. **198**, 111 (1998).

[10] T. Koma, H. Tasaki, Phys. Rev. Lett. **74**, 3916 (1995).

[11] J. Kaupužs, Int. J. Mod. Phys. C **16**, 1121 (2005)

[12] J. Kaupužs, Ann. Phys. (Leipzig) **10**, 299 (2001)

[13] T. Hara, private communication

[14] G. Parisi, Cargése Lectures 1973, published in J. Stat. Phys. **23**, 49 (1980)

[15] E. Brézin, J. C. Le Guillou, J. Zinn–Justin, in *Phase Transitions and Critical Phenomena*, edited by C. Domb, and M. S. Green (Academic, New York, 1976), Vol. 6.

[16] J. C. LeGuillou, J. Zinn–Justin, Phys. Rev. Lett. **39**, 95 (1977)

[17] G. A. Baker, B. G. Nickel, M. S. Green, D. I. Meiron, Phys. Rev. Lett., **36**, 1351 (1976)

[18] G. A. Baker, B. G. Nickel, D. I. Meiron, Phys. Rev. B, **17**, 1365 (1978)

[19] A. Pelissetto, E. Vicari, Physics Reports **368**, 549 (2002)